Czech Technical University in Prague
Faculty of Nuclear Sciences and Physical Engineering

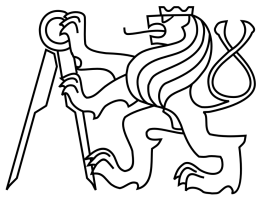

Sequential Monte Carlo methods for optimal control design

Research project

Author: Miroslav Zima
Supervisor: Ing. Václav Šmídl , Ph.D
Year: 2010

Declaration

I declare that I have written my research project myself and I have used only cited materials.

In Prague .....

.....
Miroslav Zima

Acknowledgment

I would like to thank to my supervisors Ing. Václav Šmídl, Ph.D for helpful and inspiring guidance. I have greatly benefited from his insight and assistance which helped to develop this project.

Miroslav Zima

Title:
Sequential Monte Carlo methods for optimal control design

Author: Miroslav Zima

Specialization: Mathematical Engineering
Supervisor: Ing. Václav Šmídl , Ph.D
Institute of Information Theory and Automation, Academy of Sciences of the Czech Republic

Abstract: This project deals with sequential Monte Carlo methods and especially with their usage inside framework of optimal control under uncertainty. As is shown, sequential Monte Carlo methods can be utilized for estimating. Dealing with optimal control, various techniques of controlling are discussed. Then, mentioned methods are applied on a model of permanent magnet synchronous machine drive. On this particular system, new regulator, based on cautious and dual control principles is presented obtaining better results than with conventionally used PID regulator.

Key words: Estimation, sequential Monte Carlo method, optimal control under uncertainty

Contents

List of abbreviations

ASIR	Auxiliary Sequential Importance Sampling
CC	Cautious Control
CEC	Certainty Equivalence Control
EKF	Extended Kalman Filter
IS	Importance Sampling
KF	Kalman Filter
OLFC	Open Loop Feedback Control
PF	Particle Filter
PID	Proportional Integral Derivative
PI	Proportional Integral
PMSM	Permanent Magnet Synchronous Machine
SIDP	Stochastic Iterative dynamic programming
SIR	Sequential Importance Resampling
SIR_{opt}	Sequential Importance Resampling with optimal importance distribution
$\text{SIR}_{\text{prior}}$	Sequential Importance Resampling with prior importance distribution
SIS	Sequential Importance Sampling
SMC	Sequential Monte Carlo

Introduction

In wide range of subjects, we are dealing with a problem of making inferences about a hidden state of a dynamical stochastic system using only noisy observations. This framework occurs for instance in finance [15], signal processing [9], or control theory under uncertainty [26]. Due to the system dynamics, we would like to make inferences sequentially every time where a measurement is received, thus in a form of some recursive filter. A recursive filtering approach means that received data are processed sequentially rather than as a batch so that it is not necessary to store the complete data set nor to reprocess existing data if a new measurement becomes available. Process of estimation is usually done in two stages: prediction and update. In the prediction stage, an estimate available in current time is propagated using the system model and the observation model. The estimate is then updated through Bayes rule by comparing predicted and measured values.

If the system is linear with Gaussian noise, the optimal estimator can be computed analytically as so called Kalman filter [18]. In more general cases, the optimal solution does not have a closed form and, as consequence, some approximation technique have to be used. For example, extended Kalman filter utilizes local linearization of the system. Nonetheless, in highly nonlinear cases, the approximation proposed by linearization technique may be inaccurate. This disadvantage can be lowered by using the so called unscented Kalman filter [16]. However, Kalman filter and all its derivatives are based on Gaussian noise assumption and the provided filtering density is also Gaussian. This can be limiting in various applications.

Another approach lies in so called particle filters. Particle filters belongs to the class of simulation filters which recursively approximate a filtering distribution by a cloud of points or 'particles' with point mass distribution. This is a principle of sequential Monte Carlo methods. Main advantage of particle filters is that they are not based on any assumption on linearity of the system or Gaussian distributions, so they can be used in various applications where a standard approach based on Kalman filter suffers.

The topic of this research project is to review known approaches to particle filtering. Particle filters are then applied on particular problem in problematics of optimal control under uncertainty.The problem of optimal control is formulated in the first chapter showing that it consist of two subproblems: 1) to estimate uncertain parameters of the system which is to be controlled and 2) to make a decision which results in desired system behavior. The estimation problem is the subject of the second chapter while the third chapter deals with the problem of decision making

under uncertainty. The fourth chapter includes both application and comparison of reviewed methods on a model of permanent magnet synchronous machine drive. Furthemore, new successful regulator based on cautious and dual control principles is outlined for the model.

Chapter 1

Optimal control problem

In both technical applications and real life, we are tended to making decisions which should be based on knowledge about a system of interest. If we would like to control the system successfully, we are dealing with two subproblems: 1) to observe the system and 2) to design a control action which leads to a desired system behavior. However, these two subproblems are often in a conflict - better knowledge about the system is obtained when its behavior is unexpected. Moreover, if a noise is presented, our knowledge will not be ever absolute.

This chapter aims to a mathematical formulation of the optimal control problem. The problem is then decomposed into filtering and decision making which are discussed in respective chapters.

1.1 Problem formulation

In control theory [3], it is convention to describe a dynamical system by means of a time discrete state-space model. We consider a Markovian state-space model given by

$$x_t = f_t(x_{t-1}, u_{t-1}) + w_{t-1} \qquad t \geq 1, \tag{1.1}$$

where t is time index, $x_t \in \mathbb{R}^{n_x}$ is the state of the system, $u_t \in U_t \subset \mathbb{R}^{n_u}$ is the control action , $w_t \in \mathbb{R}^{n_w}$ is i.i.d. random variable and $f_t : \mathbb{R}^{n_x} \times \mathbb{R}^{n_u} \to \mathbb{R}^{n_x}$ are arbitrary known functions. An initial state x_0 is assumed to be distributed according to some prior density $p(x_0)$. Information about the system are provided by an observation

$$y_t = h_t(x_t) + v_t \qquad t \geq 0, \tag{1.2}$$

here $y_t \in \mathbb{R}^{n_y}$ is the observation, $v_t \in \mathbb{R}^{n_v}$ is i.i.d. random variable and $h_t : \mathbb{R}^{n_y} \times \mathbb{R}^{n_v} \to \mathbb{R}^{n_y}$ are arbitrary known functions.

Suppose, that we are interested in the system control within a control horizon $0 : n$. Then, the aim is to design a control sequence $u_{0:n-1}$, which will lead to the desired system behavior. For determination how accurate is some proposed control sequence, a known real function $g(x_{1:t}, u_{0:n-1})$, called loss function, is adopted.

Due to the noise presence and the fact that we can observe only y_t, the loss function can not be evaluated directly, thus we are interested in its expectation

$$J = \mathrm{E}\{g(x_{1:t}, u_{0:t-1})\}. \tag{1.3}$$

Finally, the problem of optimal control is to minimize the expectation loss (1.3) with respect to $u_{0:t-1} \in U_{0:t-1}$.

1.1.1 Sequential parameter estimation

According to the system (1.1) and the observation (1.2), the model can be viewed as a hidden Markov model described by (without any loss of generality, we omit the dependence on u_t)

$$p(x_t|x_{t-1}) \qquad t \geq 0, \tag{1.4}$$
$$p(y_t|x_t) \qquad t \geq 0, \tag{1.5}$$

where we denote $p(x_0) := p(x_0|x_{-1})$ for notation convenience.

The aim of the estimation in time t is to compute $p(x_{0:t}|y_{0:t})$ and the expectation

$$\mathrm{E}\{g_t\} = \int g_t(x_{0:t}) p(x_{0:t}|y_{0:t}) dx_{0:t} \tag{1.6}$$

for any $p(x_{0:t}|y_{0:t})$ integrable function $g_t : \mathbb{R}^{(t+1)\times n_x} \to \mathbb{R}$. Particularly, we will be interested in computation of marginal $p(x_t|y_{0:t})$.

1.1.2 Decision making

Generally, the decision making can be done in two different ways. At first, whole action sequence can be computed off-line and, as a consequence, there is no gain from feedback of the system during simulations. This approach, called open-loop control, is reasonable only in cases where measurements are not available or are unreliable. This case is off our interest.

In a closed-loop approach, the control actions are computed on-line. It means, that u_{t-1} is computed based on current estimate of x_{t-1} which is sequentially update using the measurement y_t. This situation is schematically depicted in figure 1.1 In time-critical applications, it is necessary to have some computational effective formula for the control action. This parametric formula is usually computed off-line and only evaluation using respective values is performed on-line.

Of course, control sequence proposed by any parametric formula along control horizon should minimize the expectation loss (1.3). Even if we be able to compute expectation loss for every $u_{0:t-1} \in U_{0:t-1}$, direct minimization over action space $U_{0:t-1}$ will be impossible already for very simple problems. Due to this complications, many approximation techniques or problem specifications have been proposed,

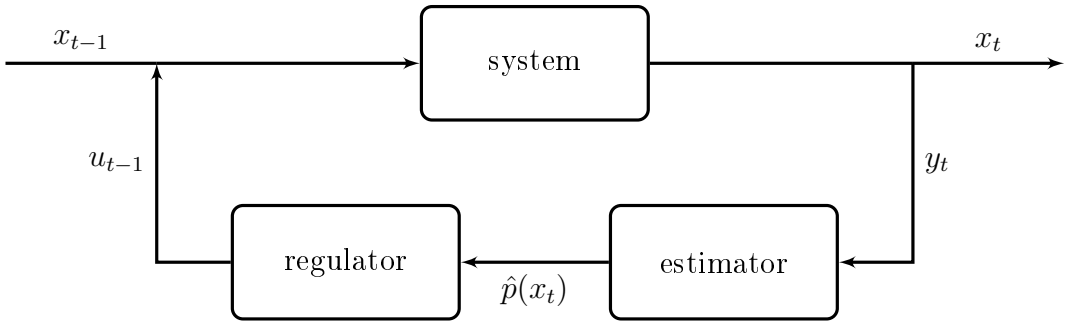

Figure 1.1: Close-loop control.

some general approaches are presented in corresponding chapter. Using an approximation of optimal control, it is often crucial to use closed-loop control because we can evaluate how the proposed control action leads to the desired state and possibly tune the parametric formula to be more effective. On this very simple (but powerful) idea is based e.g. PID regulator [17].

Chapter 2

Sequential parameter estimation

In this chapter, we present a general framework for sequential parameter estimation. The main interest lies in sequential Monte Carlo approach. For a later comparison, a Kalman filter based techniques are also briefly presented.

2.1 Parameter estimation with perfect Monte Carlo simulation

Before we induce sequential Monte Carlo methods, we briefly introduce a traditional Monte Carlo approach. Suppose, that the aim is to estimate an expectation for function $g_t : \mathbb{R}^{(n+1)\times n_x} \to \mathbb{R}$

$$\mathrm{E}\{g_t\} = \int g_t(x_{0:t}) p(x_{0:t}|y_{0:t}) dx_{0:t} \tag{2.1}$$

The idea of the traditional Monte Carlo method is to approximate density $p(x_{0:t}|y_{0:t})$ by an empirical estimate

$$\hat{p}(x_{0:t}|y_{0:t}) = \frac{1}{N} \sum_{i=1}^{N} \delta(x_{0:t} - x_{0:t}^{(i)}), \tag{2.2}$$

where $\{x_{0:t}^{(i)}\}_{i=1}^{N}$ are random samples drawn from density $p(x_{0:t}|y_{0:t})$ and δ is the Dirac delta function. The Monte Carlo estimate is obtained by substituting the approximation (2.2) into (2.1), thus

$$\mathrm{E}\{g_t\} \approx \hat{\mathrm{E}}\{g_t\} = \int g_t(x_{0:t}) \hat{p}(dx_{0:t}|y_{0:t}) dx_{0:t} = \frac{1}{N} \sum_{i=1}^{N} g_t(x_{0:t}^{(i)}). \tag{2.3}$$

Due to the strong law of large numbers, $\hat{\mathrm{E}}(g_t)$ converges to $\mathrm{E}(g_t)$ almost surely and, if variance σ of $g_t(x_{0:t})$ is finite, central limit theorem holds

$$\sqrt{N}(\hat{\mathrm{E}}(g_t) - \mathrm{E}(g_t)) \to \mathcal{N}(0, \sigma^2) \qquad \text{if } N \to \infty. \tag{2.4}$$

The major problem of this approach is the assumption that we can sample from density $p(x_{0:t}|y_{0:t})$.

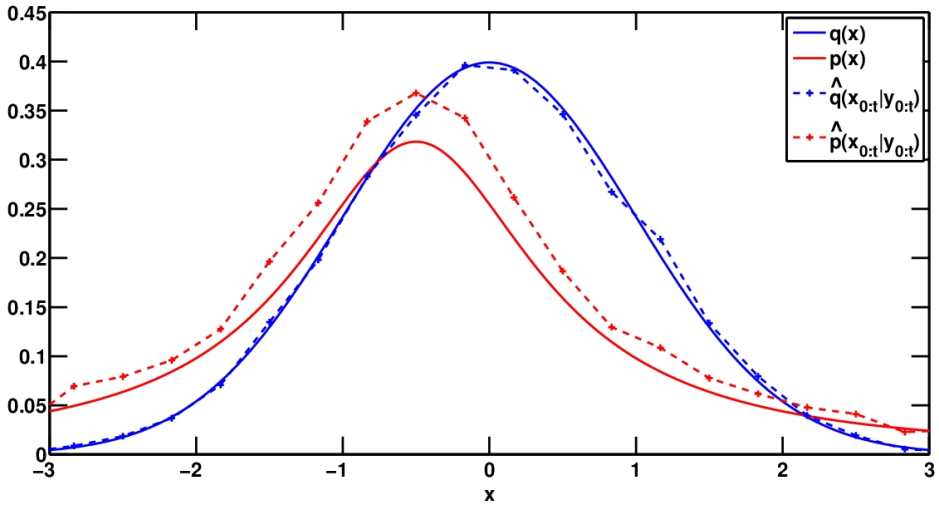

Figure 2.1: Using the IS, original density $p(x_{0:t}|y_{0:t})$ is approximated by $\hat{p}(x_{0:t}|y_{0:t})$ which is realized by weighted samples $\{x_{0:t}^{(i)}\}_{i=1}^{N}$ drawn from importance density $q(x_{0:t}|y_{0:t})$. Because the probability distribution outside interval covered by particles is not taken into account in the approximation, the IS estimate overestimates the probability distribution inside the interval. Here, 10000 samples is used

2.2 Importance sampling

Another approximation of expectation (2.1) can be done using Importance Sampling (IS) method [12]. Unlike the previous method, the IS method works even if we can not sample from density $p(x_{0:n}|y_{0:n})$. The idea of the IS method is to use a well known density $q(x_{0:n}|y_{0:n})$, so called importance density, instead of $p(x_{0:n}|y_{0:n})$, see figure 2.1. If a support of $q(x_{0:n}|y_{0:n})$ includes a support of $p(x_{0:n}|y_{0:n})$, the expectation can be expressed as

$$\mathrm{E}\{g_t\} = \int g_t(x_{0:t})p(x_{0:t}|y_{0:t})dx_{0:t} = \frac{\int g_t(x_{0:n})\omega(x_{0:t})q(x_{0:t}|y_{0:t})dx_{0:t}}{\int \omega(x_{0:t})q(x_{0:t}|y_{0:t})dx_{0:t}}, \tag{2.5}$$

where importance weighs $\omega(x_{0:t})$ are defined as

$$\omega(x_{0:t}) = \frac{p(x_{0:t}|y_{0:t})}{q(x_{0:t}|y_{0:t})}. \tag{2.6}$$

The Monte Carlo estimate can be obtained by using random samples $\{x_{0:t}^{(i)}\}_{i=1}^{N}$ drawn from importance density $q(x_{0:t}|y_{0:t})$ in (2.5)

$$\hat{\mathrm{E}}(g_t) = \frac{\frac{1}{N}\sum_{i=1}^{N} g_t(x_{0:t}^{(i)})\omega_t^{(i)}}{\frac{1}{N}\sum_{i=1}^{N}\omega_t^{(i)}} = \sum_{i=1}^{N} g_t(x_{0:t}^{(i)})\tilde{\omega}_t^{(i)}, \tag{2.7}$$

where the normalized importance weighs $\tilde{\omega}_t^{(i)}$ are

$$\tilde{\omega}_t^{(i)} = \frac{\omega_t^{(i)}}{\sum_{i=1}^{N}\omega_t^{(i)}} = \frac{\omega(x_{0:t}^{(i)})}{\sum_{i=1}^{N}\omega(x_{0:t}^{(i)})} \tag{2.8}$$

Again, due to the strong law of large numbers, the estimate $\hat{p}(dx_{0:t}|y_{0:t})$ based on $\hat{q}(dx_{0:t}|y_{0:t})$ and $\{\tilde{\omega}_t^{(i)}\}_{i=1}^N$ converges to the true posterior density $p(dx_{0:t}|y_{0:t})$ and also estimated expectation $\hat{\mathrm{E}}(g_t)$ converges to the $\mathrm{E}(g_t)$ if N tends to infinity .

The disadvantage of this approach is that we need to evaluate $p(x_{0:t}^{(i)}|y_{0:t})$ and the importance weights have to be recomputed over the entire state sequence. Consequently, computational complexity increases in time.

2.3 Sequential importance sampling

For $p(x_{0:t}|y_{0:t})$, it can be derived

$$\begin{aligned} p(x_{0:t}|y_{0:t}) &= \frac{p(y_t|x_{0:t}, y_{0:t-1})p(x_{0:t}|y_{0:t-1})}{p(y_t|y_{0:t-1})} \\ &= \frac{p(y_t|x_{0:t}, y_{0:t-1})p(x_{0:t}|y_{0:t-1})}{p(y_t|y_{0:t-1})} \\ &= \frac{p(y_t|x_{0:t}, y_{0:t-1})p(x_t|x_{0:t-1}, y_{0:t-1})p(x_{0:t-1}|y_{0:t-1})}{p(y_t|y_{0:t-1})} \\ &= \frac{p(y_t|x_t)p(x_t|x_{t-1})p(x_{0:t-1}|y_{0:t-1})}{p(y_t|y_{0:t-1})}, \end{aligned}$$

where first two equalities follow from Bayesian rule, third from definition of conditional distribution, and the last one from Markovian property. Thus, the density satisfies a recursive formula

$$p(x_{0:t}|y_{0:t}) \propto p(y_t|x_t)p(x_t|x_{t-1})p(x_{0:t-1}|y_{0:t-1}). \tag{2.9}$$

For derivation a recursive formula for importance weights, it is suitable to have an importance density which satisfies

$$q(x_{0:t}|y_{0:t}) = q(x_t|x_{0:t-1}, y_{0:t-1})q(x_{0:t-1}|y_{0:t-1}). \tag{2.10}$$

In this particular case, the $x_{0:t}^{(i)}$ is formed as $x_{0:t}^{(i)} = (x_{0:t-1}^{(i)}, x_t^{(i)})$, where $x_t^{(i)}$ is drawn from $q(x_t|x_{0:t-1}^{(i)}, y_{0:t-1})$. The importance weights for every $x_{0:t}^{(i)}$ can be computed sequentially as

$$\omega_t^{(i)} \propto \omega_{t-1}^{(i)} \frac{p(y_t|x_t^{(i)})p(x_t^{(i)}|x_{t-1}^{(i)})}{q(x_t^{(i)}|x_{0:t-1}^{(i)}, y_{0:t-1})}, \tag{2.11}$$

what gives the Sequential Importance Sampling (SIS) filter, see scheme 2.1. The approximation $\hat{\mathrm{E}}(g_t)$ of the expectation $\mathrm{E}(g_t)$ can be computed according to (2.7).

The advantage of using the SIS filter is that it is sufficient to sample only $x_t^{(i)}$ instead of whole $x_{0:t}^{(i)}$ and we do not have to evaluate $p(x_{0:t}^{(i)}|y_{0:t})$.

2.4 Degeneracy of the SIS filter

For good performance of the SIS filter, it is suitable to have the importance density $q(x_{0:t}|y_{0:t})$ close to the true posterior distribution $p(x_{0:t}|y_{0:t})$. However, as can be

Algorithm 2.1 Sequential Importance Sampling

for $t = 1, 2, \ldots$ **do**
  for $i = 1$ to N **do**
    sample $x_t^{(i)}$ from $q(x_t|x_{0:t-1}^{(i)}, y_{0:t-1})$
    set $x_{0:t}^{(i)} = (x_{0:t-1}^{(i)}, x_t^{(i)})$
  end for
  for $i = 1$ to t **do**
    compute importance weights using recursive formula

$$\omega_t^{(i)} = \omega_{t-1}^{(i)} \frac{p(y_t|x_t)p(x_t|x_{t-1})}{q(x_t|x_{0:t-1}, y_{0:t-1})}$$

  end for
  for $i = 1$ to N **do**
    normalize importance weights

$$\tilde{\omega}_t^{(i)} = \frac{\omega_t^{(i)}}{\sum_{i=1}^{N} \omega_t^{(i)}}$$

  end for
end for

seen from following proposition, the variance of importance weights can only increase over time.

Proposition 1. *The variance of importance weights with both $x_{0:t-1}$ $y_{0:t}$ interpreted as random variables increases over time.*

The variance of importance weights can be reduced by using proper importance density; the optimal one is stated in the next proposition.

Proposition 2. *The importance density which minimizes the variance of the importance weight $\omega_t^{(i)}$ conditional upon $x_{0:t-1}^{(i)}$ and $x_{0:t-1}^{(i)}$ is $q(x_t|x_{0:t-1}, y_{0:t}) = p(x_t|x_{t-1}, y_t)$.*

Both presented propositions are taken from [8].

Using the optimal density in (2.11), the updating procedure for weights will have the form $\omega_t^{(i)} = \omega_{t-1}^{(i)} p(y_t|x_{t-1}^{(i)})$. However, the optimal density has two major drawbacks: 1) it requires the ability of sampling from $p(x_t|x_{t-1}, y_t)$, and 2) to calculate $p(y_t|x_{t-1}^{(i)})$. Second term can be principally evaluated using Chapman-Kolmogorov equation which, due to Markov property, has the form

$$p(y_t|x_{t-1}^{(i)}) = \int p(y_t, x_t|x_{t-1}^{(i)})dx_t = \int p(y_t|x_t, x_{t-1})p(x_t|x_{t-1}^{(i)})dx_t =$$
$$= \int p(y_t|x_t)p(x_t|x_{t-1}^{(i)})dx_t.$$

Both $p(x_t|x_{t-1}, y_t)$ and $p(y_t|x_{t-1}^{(i)})$ can be calculated for a nonlinear system with a linear observation and Gaussian noise, see [8]. However in a general case, it is not

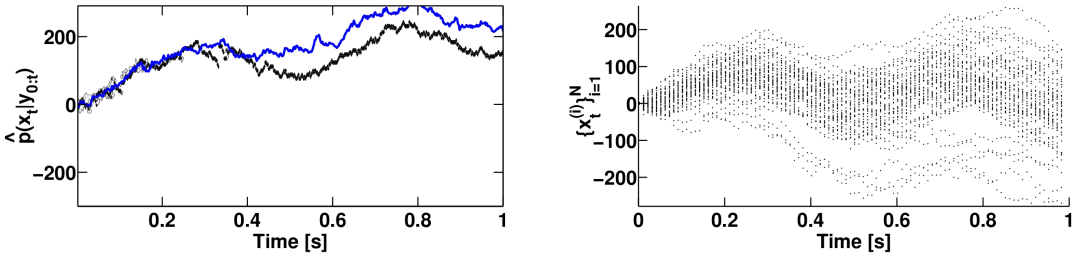

Figure 2.2: Example of degeneracy phenomenon using the SIS filter. The left part shows estimated state x_t in particular time, darker color means higher probability. True state is marked by blue line. All the particles in the corresponding times are depicted in the right part. The number of particles is $N = 50$.

possible and some approximation have to be utilized. A suitable choice can be e.g. usage of local linearization [8] or prior distribution [24]. This topic, crucial to limit the degeneracy, is discussed in respective chapter on examples.

In practice after few iterations, the majority of the normalized importance weights is close to zero due to the degeneracy of the SIS filter, see figure 2.2. Consequently, the major of computation effort is devoted inefficiently to trajectories whose probability is almost zero. Furthermore, any inferences based on these samples will be inaccurate. To overcome this drawback, the resampling procedure is used.

2.5 Resampling

The idea of the resampling procedure is to eliminate particles with small normalized weights and to use copies of the others. In other words, the resampling step produces new particles $\{x_{0:t}^{*(i)}\}_{i=1}^N$ and corresponding weights $\{\tilde{\omega}_t^{*(i)}\}_{i=1}^N$ based on $\{x_{0:t}^{(i)}\}_{i=1}^N$ and $\{\tilde{\omega}_t^{(i)}\}_{i=1}^N$, see2.3 as an example. The mechanism, how the new particles are produced, depends on used resampling scheme, see [6] and [14] for overview. All resampling procedures discussed below use $\tilde{\omega}_t^{*(i)} = 1/N$. Due to the fact that $x_{0:t}^{(i)} = (x_{0:t-1}^{(i)}, x_t^{(i)})$, the resampling procedure is performed only with respect to $x_t^{(i)}$. Remaining part $x_{0:t-1}^{*(i)}$ is determined accordingly to $x_t^{*(i)}$.

2.5.1 Multinomial resampling

Multinomial resampling, discussed in [24], uses $\{x_t^{*(i)}\}_{i=1}^N$ drawn from point mass distribution $\sum_{i=1}^N \tilde{\omega}_t^{(i)} \delta(x_t - x_t^{(i)})$ where δ is the Dirac delta function. Practical implementation of multinomial resampling uses samples drawn from uniform distribution $U((0;1])$ which determines $N^{(i)}$, the numbers of identical copies of the original sample $x_{0:t}^{(i)}$. Multinomial resampling is summarized in scheme 2.2.

Algorithm 2.2 Multinomial resampling

for $i = 1$ to N **do**
  compute the cumulative weights $\widehat{\omega}_t^{(i)} = \sum_{j=1}^{i} \tilde{\omega}_t^{(j)}$
end for
for $i = 1$ to N **do**
  sample U^i from uniform distribution $U((0;1])$
end for
order $\{U^{(i)}\}_{i=1}^{N}$ in ascending order
for $i = 1$ to N **do**
  compute $N^{(i)}$ satisfies $\sum_{j=1}^{i} N^{(j)} = \max_{0 \geq l \geq N}\{l | \widehat{\omega}_t^{(i)} > U^{(i)}\}$
end for
for $i = 1$ to N **do**
  for $j = i$ to $i - 1 + N^{(i)}$ **do**
    state $x_{0:t}^{*(i+j)} = x_{0:t}^{(i)}$
  end for
end for

2.5.2 Residual resampling

In residual resampling [13], the number of identical copies for the original sample $x_{0:t}^{(i)}$ is set to $\tilde{N}^{(i)} = \lfloor N\tilde{\omega}_t^{(i)} \rfloor$ for each i. The rest $N - \sum_{j=1}^{N} \tilde{N}^{(j)}$ particles si computed using any other resampling scheme. For example by multinomial resampling for weights

$$\bar{\omega}_t^{(i)} = \frac{\widehat{\omega}^{(i)} N - \tilde{N}^{(i)}}{N - \sum_{j=1}^{N} \tilde{N}^{(j)}} \qquad i = 1, \ldots, N. \tag{2.12}$$

Another possible choice for second step of residual resampling is to use one additional copy for first $N - \sum_{j=1}^{N} \tilde{N}^{(j)}$ particles ordered according to $Ni - \tilde{N}^{(i)}$. By this choice, we obtain a completely deterministic version of the resampling procedure.

Residual resampling proceeds according to scheme 2.3.

Algorithm 2.3 Residual resampling

for $i = 1$ to N **do**
  compute $\tilde{N}^{(i)} = \lfloor N\tilde{\omega}_t^{(i)} \rfloor$
end for
for $i = 1$ to N **do**
  set altered weights according to (2.12)
end for
for $i = 1$ to $\sum_{j=1}^{N} \tilde{N}^{(j)}$ **do**
  for $j = i$ to $i - 1 + \tilde{N}^{(i)}$ **do**
    state $x_{0:t}^{*(i+j)} = x_{0:t}^{(i)}$
  end for
end for
get rest $N - \sum_{j=1}^{N} \tilde{N}^{(j)}$ particles from multinomial resampling for $\{x_{0:t}^{(i)}, \bar{\omega}_t^{(i)}\}_{i=1}^{N}$.

It can be shown (e.g. [6]) that the conditional variance of residual sampling is always

smaller than that of multinomial sampling.

2.5.3 Systematic resampling

Systematic resampling [19] needs only one sample U drawn from uniform distribution $U((0;1/N])$. The numbers of copies $\{N^{(i)}\}_{i=1}^{N}$ are computed similarly to multinomial resampling schemes using equidistant values

$$U^{(i)} = U + \frac{l-1}{N} \qquad i = 1, 2, \ldots, N. \tag{2.13}$$

Although due to only one random sample needed, systematic resampling is less computationally expensive than previous methods, each resampling particles are (conditionally) dependent and they are sensitive on permutation of the original ones. Thus, studying of systematic resampling method is much harder than for other methods.

2.5.4 Regularized resampling

Using samples from point mass distribution $\sum_{i=1}^{N} \tilde{\omega}_t^{(i)} \delta(x_t - x_t^{(i)})$, it is possible that after resampling step, many particles will have no descendants. In the extreme case, there will be only one type of particles obtained from a single one. A possible approach to overcome this impoverishment of diversity is to use regularized resampling [7]. In regularized resampling, instead of the point mass distribution a continuous approximation of posterior distribution is used

$$\hat{p}(x_t|y_{1:t}) = \sum_{i=1}^{N} \tilde{\omega}_t^{(i)} K(\frac{x_t - x_t^{(i)}}{b}). \tag{2.14}$$

Here K is a kernel density function and $b > 0$ is a scalar parameter, called Kernel bandwidth. The Kernel density is a symmetric function with zero mean and finite variance. The kernel K and the parameter b are optimally chosen as minimizers of mean square error between the posterior density and its approximation (2.14) defined as

$$\mathrm{E}\left[\int \hat{p}(x_t|y_{1:t}) - p(x_t|y_{1:t})\right], \tag{2.15}$$

where E is the expectation evaluated with respect to the samples. In the particular case with equal normalized weights, the optimal kernel is the Epanechnikov kernel [10]

$$K_{opt} = \begin{cases} \frac{n_x+2}{2c_{n_x}}(1 - ||x||^2) & \text{if } ||x|| < 1, \\ 0 & \text{otherwise,} \end{cases} \tag{2.16}$$

where c_{n_x} is volume of unit sphere in $\mathbf{R}^{n_x}$. Additionally, if the distribution is Gaussian with unit covariance matrix, the corresponding bandwidth is

$$h_{opt} = \left[\frac{8(n_x+4)(2\sqrt{\pi})^{n_x}}{c_{n_x}}\right]^{\frac{1}{n_x+4}}. \tag{2.17}$$

Due to easy computation and good performance in empirical simulations (e.g. [25]), this bandwidth is used even in non Gaussian cases. Consequently, regularized resampling can be performed by the algorithm summarized in scheme 2.4.

Algorithm 2.4 Regularized resampling

for $\{x_t^{(i)}, \tilde{\omega}_t^{(i)}\}_{i=1}^N$ calculate the empirical covariance S_t
perform decomposition $D_t D_t^T = S_t$
get $\{\tilde{x}_t^{*(i)}\}_{i=1}^N$ as a resample of $\{x_t^{(i)}\}_{i=1}^N$ using any resampling procedures
for $i = 1$ to N **do**
  draw $e^{(i)} \sim K_{opt}$
  regularize $x_t^{*(i)} = \tilde{x}_t^{*(i)} + b_{opt} D_t e^{(i)}$
end for

2.6 Sequential importance resampling

Sequential Importance Resampling (SIR) filter is obtained by usage of any resampling procedure in the original SIS filter when degeneracy of the SIS filter is above some certain threshold. One of first particle filters of this type was so called bootstrap filter [24] which utilized prior density as importance density and multinomial resampling after each step.

For estimating a level of the degeneracy (and as a criterion for usage of a resampling procedure) an effective sample size introduced in [20] is used

$$N_{eff} = \frac{N}{1 + \mathrm{Var}(\omega(x_{0:t}))}. \tag{2.18}$$

Exact evaluation of N_{eff} is impossible but an estimate $\widehat{N_{eff}}$ based on computed $\omega_t^{(i)}$ is given by

$$\widehat{N_{eff}} = \frac{1}{\sum_{i=1}^N (\tilde{\omega}_t^{(i)})^2}. \tag{2.19}$$

The resampling step is induced whenever $\widehat{N_{eff}}$ is bellow some fixed threshold N_{tresh}, see the scheme 2.5. The adantage of using the SIR filter in the simulation from figure 2.2 is presented in figure 2.3

Despite of overcoming the degeneracy phenomenon, after resampling, particles are no longer statistically independent. However in [4], the central limit theorem was stated at lest for scheme where resampling is used after each step. Also practical problems occur when resampling procedure is used because, in contrary to the SIS filter, SIR filter is not fully paralellizable since during resampling all particles are combined.

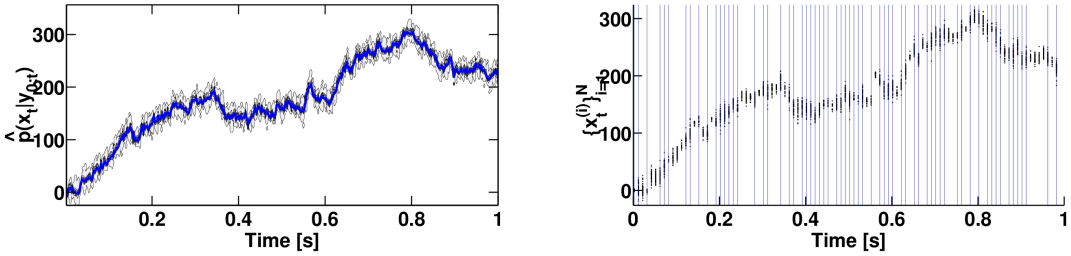

Figure 2.3: Simulation from the figure 2.2 where the SIS filter is replaced by the SIR filter. If the importance weights are distributed very unevenly (marked by blue lines in the right part), the resampling step is used for overcoming the degeneracy. Here, multinomial resampling with $N_{thresh} = N/5 = 12$ is used.

Algorithm 2.5 Sequential Importance Resampling

---

for $t = 1, 2, \ldots$ **do**

update $\{x_{0:t-1}^{(i)}, \tilde{\omega}_{t-1}^{(i)}\}_{i=1}^{N}$ to $\{x_{0:t}^{(i)}, \tilde{\omega}_{t}^{(i)}\}_{i=1}^{N}$ using one step of the SIS filter

compute an estimate of effective sample size

$$\widehat{N_{eff}} = \frac{1}{\sum_{i=1}^{N} (\tilde{\omega}_t^{(i)})^2}.$$

if $\widehat{N_{eff}} < N_{tresh}$ **then**

update $\{x_{0:t}^{(i)}, \tilde{\omega}_{t}^{(i)}\}_{i=1}^{N}$ to $\{x_{0:t}^{*(i)}, \tilde{\omega}_{t}^{*(i)}\}_{i=1}^{N}$ using a resampling procedure

end if

end for

2.7 Auxiliary sampling importance resampling

The goal of Auxiliary Sampling Importance Resampling (ASIR) filter, presented in [23], is to design a variant of the SIR filter which would be more robust against outliers. The main idea is to use a higher dimensional importance density $q(x_t, i|y_{1:t})$ from which are sampled pairs of $\{x_t^{(i)}, i^j\}_{i=1}^N$. Here, i^j denotes an index of an antecedent particle of $x_t^{(i)}$ at iteration $t-1$. Straightforward application of Bayes rule and corresponding definitions of i and $\omega_{t-1}^{(i)}$ gives

$$\begin{aligned} p(x_t, i|y_{0:t}) &= \frac{p(y_t|x_t, i, y_{0:t-1})p(x_t, i|y_{0:t-1})}{p(y_t|y_{0:t-1})} \\ &\propto p(y_t|x_t, y_{0:t-1})p(x_t, i|y_{0:t-1}) \\ &= p(y_t|x_t, y_{0:t-1})p(x_t|i, y_{0:t-1})p(i|y_{0:t-1}) \\ &= p(y_t|x_t)p(x_t|x_{t-1})\omega_{t-1}^{(i)} \end{aligned}$$

The importance density is defined to satisfy a similar proportionality

$$q(x_t, i|y_{0:t}) \propto p(y_t|\mu_t^{(i)})p(x_t|x_{t-1})\omega_{t-1}^{(i)}, \tag{2.20}$$

where $\mu_t^{(i)}$ is some characterization of x_t given $x_{t-1}^{(i)}$. A suitable choice could be e.g. mean value or random sample from $p(x_t|x_{t-1}^{(i)})$. The importance density is also chosen to satisfy

$$q(x_t|i, y_{0:t}) = p(x_t|x_{t-1}^{(i)}), \tag{2.21}$$

and thus

$$q(x_t, i|y_{0:t}) = q(i|y_{0:t})q(x_t|i, y_{0:t}). \tag{2.22}$$

Combing together with (2.20), we obtain

$$q(i|y_{1:t}) \propto p(y_t|\mu_t^{(i)})\omega_{t-1}^{(i)}. \tag{2.23}$$

Using the previous, the weights are updated according to

$$\omega_t^{(j)} = \omega_{t-1}^{(i_j)} \frac{p(x_t^{(i)}, i_j|y_{0:t})}{q(x_t^{(i)}, i|y_{0:t})} \propto \omega_{t-1}^{(i_j)} \frac{p(y_t|x_t^{(i)})}{p(y_t|\mu_t^{(i_j)})}. \tag{2.24}$$

Algorithm of the ASIR filter is summarized in scheme 2.6. Note, that it is not necessary to produce whole samples $\{x_t^{(i)}, i_j\}_{i=1}^N$.

Following previous scheme, it can be seen, that the ASIR filter is similar to the bootstrap filter [24]. Both algorithms uses the prior density as importance density and resampling procedure during each step. Motivation for the ASIR filter was to improve performance of the SIR filter in cases with outliers. The reason, why the ASIR filter is more robust, is that the algorithm performs resampling step first and then sample only with respect to particles which are most likely to be close to the true state. Consequently, the weights after importance sampling step will be distributed more evenly. However, if the process noise is large, a single point does not characterize $p(x_t|x_{t-1}^{(i)})$ well, and the ASIR filter resamples based on a poor approximation of $p(x_t|x_{t-1}^{(i)})$. In such scenarios, the use of the ASIR filter degrades performance of estimation process.

Algorithm 2.6 Auxiliary Sampling Importance Resampling

for $t = 1, 2, \ldots$ **do**
  for $i = 1$ to N **do**
    calculate $\mu_t^{(i)}$
    set $\omega_t^{(i)} \propto p(y_t|\mu_t^{(i)})\omega_{t-1}^{(i)}$
  end for
  compute normalized importance weights $\{\tilde{\omega}_t^{(i)}\}_{i=1}^N$ (from $\{\omega_t^{(i)}\}_{i=1}^N$)
  determine the $\{i_j\}_{i=1}^N$ using a resampling scheme with $\{\tilde{\omega}_t^{(i)}\}_{i=1}^N$
  for $j = 1$ to N **do**
    sample $x_t^{(j)}$ from $q(x_t|i_j, y_{0:t}) = p(x_t|x_{t-1}^{(i_j)})$
    set $x_{0:t}^{(j)} = (x_{0:t-1}^{(i_j)}, x_t^{(j)})$
  end for
  for $j = 1$ to N **do**
    compute (second stage) importance weights using

$$\omega_t^{(j)} \propto \frac{p(y_t|x_t^{(j)})}{p(y_t|\mu_t^{(i_j)})}$$

  end for
  compute normalized importance weights $\{\tilde{\omega}_t^{(i)}\}_{i=1}^N$
end for

2.7.1 Illustrative example

For a brief illustration of advantage of the ASIR filter, we consider a system described by

$$\begin{aligned} x_t &= 1.2x_{t-1} + w_{t-1} \\ y_t &= x_t + v_t \end{aligned} \qquad t = 1, \ldots, 20 \tag{2.25}$$

where $w_{t-1} \sim \mathcal{N}(0, \sigma_w^2)$, $v_t \sim \mathcal{N}(0, \sigma_v^2)$, $x_0 \sim \mathcal{N}(0, \sigma_0^2)$, $\sigma_w = 0.01$, $\sigma_v = 0.05$ and $\sigma_0 = 0.001$. In $t = 5$, the outlier is simulated by $w_4 = 0.5$. Due to the similarities depicted above, bootstrap filter is used for a comparison. Multinomial resampling was used both in the ASIR filter and the bootstrap filter. Two possible realizations are shown in figure 2.4. After 1000 simulations, mean square error using the ASIR filter was lesser of 35% than with the bootstrap filter.

More comprehensive study of the ASIR filter with illustrative examples was presented in [23].

2.8 Kalman filter based estimators

A classical approach to sequential parameter estimation is the well known Kalman filter [18]. The Kalman filter was derived as an optimal filter in a case of linear system with Gaussian noise. However, various extensions for nonlinear cases have been proposed. For later comparison, we briefly present Kalman filter and its most commonly used extension, the so called Extended Kalman filter. Till nowadays, many

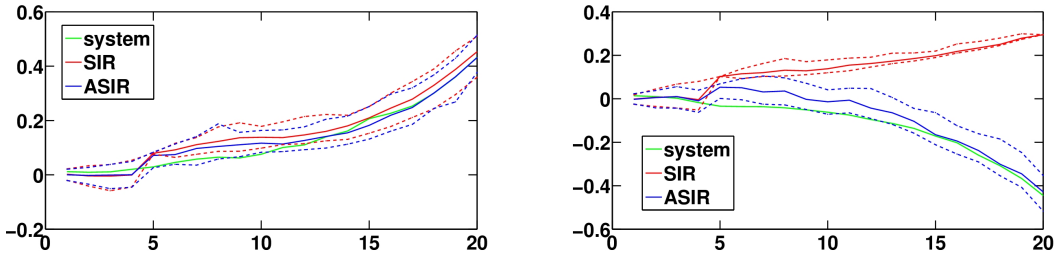

Figure 2.4: In the left part of the figure, typical realization of the scenario is presented. Dotted lines describe range of the particles. It can be seen, that the ASIR filter reduces error caused by the outlier in $t = 5$ slightly better. In extreme case, the estimation using the bootstrap filter is no longer possible, see the right part.

other extensions of the original Kalman filter has been proposed (e.g. Unscended KF [16] or Gausian Sum Filters [21]), but all of them are based on Gaussian densities, which can be limiting in particular applications.

2.8.1 Kalman filter

In 1960, the solution of optimal estimator of a linear system with Gaussian noises was derived in [18] and was named after its autor as Kalman filter. The estimator is optimal in sense of mean square error, thus the estimate $\hat{x}$ proposed by Kalman filter minimizes

$$\mathrm{E}\{(x_t - \hat{x}_t)^2 | y_{0:t}\} \tag{2.26}$$

between all possible estimators of x.

Due to the assumption of linearity, the system is described by

$$x_t = A_t x_{t-1} + B_t u_{t-1} + w_{t-1} \qquad t \geq 1, \tag{2.27}$$

$$y_t = H_t x_t + v_{t-1}, \tag{2.28}$$

where $w_t \sim \mathcal{N}(0, Q_t)$, $v_t \sim \mathcal{N}(0, R_t)$ and matrices A_t, B_t, Q_t and R_t are supposed to be known.

It was proven in [18] that the estimate of x_t based on $y_{0:t}$ is distributed according to $\mathcal{N}(\hat{x}_{t|t}, P_{t|t})$ and can be computed sequentially as

$$\hat{x}_{t|t} = \hat{x}_{t|t-1} + K_t(y_{t+1} - H_t \hat{x}_{t|t-1}), \tag{2.29}$$

where

$$\hat{x}_{t|t-1} = A_t \hat{x}_{t-1|t-1} + B_t u_{t-1}, \tag{2.30}$$

$$P_{t|t-1} = A_t P_{t-1|t-1} A_t^T + Q_t, \tag{2.31}$$

$$K_t = P_{t|t-1} H_t^T (H_t P_{t|t-1} H_t^T + R_t)^{-1}, \tag{2.32}$$

$$P_{t|t} = (I - K_t H_t) P_{t|t-1}. \tag{2.33}$$

Although very strict assumptions udner which the Kalman filter is the optimal estimator, it is still widely used in applications, e.g. [29].

2.8.2 Extended Kalman filter

If the system is nonlinear, Kalman filter can be still used on linearized system. This straightforward extension is called the Extended Kalman Filter (EKF). Suppose, that the system is described as

$$x_f = f_t(x_{t-1}, u_{t-1}) + w_{t-1}, \tag{2.34}$$
$$y_t = h_t(x_t) + v_t, \tag{2.35}$$

where $w_t \sim \mathcal{N}(0, Q_t)$,$v_t \sim \mathcal{N}(0, R_t)$ and both functions f_t, h_t and matrices Q_t, R_t are supposed to be known.

The EKF is obtained simply from the original KF by replacing (2.29) and (2.30) by

$$\hat{x}_{t|t} = \hat{x}_{t|t-1} + K_t(y_{t+1} - h_t(\hat{x}_{t|t-1})), \tag{2.36}$$
$$\hat{x}_{t|t-1} = f_t(\hat{x}_{t-1|t-1}, u_{t-1}) \tag{2.37}$$

where the rest of the EKF uses equations from the KF with

$$A_t = \frac{\partial f}{\partial x}\Big|_{x=\hat{x}_{t-1|t-1}, u_{t-1}}, \tag{2.38}$$
$$H_t = \frac{\partial f}{\partial u}\Big|_{x=\hat{x}_{t|t-1}}, \tag{2.39}$$
$$\tag{2.40}$$

The EKF is useful especially in cases of weak nonlinearities or if the linearizing point is near to the true state. In both mentioned cases, the linearization is sufficiently accurate and the EKF often estimates the true state well. In other cases, the convergence of EKF estimates to the true state is not guaranteed. Also, EKF suffers if the true posterior density is far from the Gaussian.

Chapter 3

Decision making

The original problem of the optimal control, summarized in the minimization of (1.3), is practically unsolvable. Reasonable specification (with perspective to various applications) is to assume the loss function being additive over time, thus

$$g(x_{1:N}, u_{0:N-1}) = \sum_{t=0}^{N-1} g_t(x_{t+1}, u_t). \tag{3.1}$$

for some known real functions g_t. Under the assumption of additivity, the expectation loss can be written as

$$J(x_0) = \mathrm{E}_{w_{0:N-1}} \left\{ \sum_{t=0}^{N-1} g_t(x_{t+1}, u_t(x_t)) \right\}. \tag{3.2}$$

As was pointed out in [11], the minimization of additive loss can be (theoretically) done by dynamic programming. Dynamic programming is based on optimality principle which states that the loss $J(x_0)$ on horizon N will be minimal if and only if all losses $J_k(x_k)$ on horizon $N-k$ will by minimal. Thus, the original problem can be rewritten as a recursive problem

$$\begin{aligned} J_N(x_N) &= 0, \\ J_t(x_t) &= \min_{u_t \in U(x_t)} \mathrm{E}_{w_t} \left\{ g_k(x_{t+1}, u_t) + J_{t+1}(x_{t+1}) \right\}, \qquad t = 0, \ldots, N-1. \end{aligned} \tag{3.3}$$

Consequently, the minimization proceeds in backward direction for $k = N, \ldots, 0$ storing u_k for all possible x_k.

3.1 Optimal regulator

An optimal regulator proposes control policy (i.e. the sequence $\{u_{0:N-1}\}$) which minimizes the expectation loss (3.2). The optimal policy do not have to exist or to be unique, the sufficient condition is for example compactness of U and convexity of expectation loss J. However, analytical approach often suffers even for very simple system.

The exact solution is known for linear systems with a quadratic loss and Gaussian densities as so called Linear Quadratic Gaussian control (LQG), see [3]. The LQG control consist from Kalman filter (optimal Linear Quadratic Estimator, LQE) and Linear Quadratic Regulator (LQR).

In more general cases, both expectation and minimization can be performed only by some approximation technique.

3.2 Dual control

In [11], it was discussed that an optimal control policy should not only to control the system to the desired state, it should also have some probing ability which provide better system identification and, as consequence, allow more accurate control actions in future steps. These two requirements on the optimal policy are often in contradiction and this is what gives the name dual control. This principle could be very helpful in suboptimal control policy design – for example, if we have some control policy $u_t(x_t)$ which does not satisfies the duality principle, we can incorporate the probing term by defining a new policy as

$$\tilde{u}_t = u_t + u_t^{\text{prob}}, \tag{3.4}$$

where u_t^{prob} is the probing term. In some cases, reasonable choice for probing term can be scaled white noise.

3.3 PID regulator

A PID regulator in its standard form proposes control actions composed from proportional, integral and derivative terms which gives the abbreviation PID. This regulator is well known since early 20th century and is the most widely used controller in a process control until today [1]. The reason for its wide usage is simplicity and good performance in various applications.

The PID regulator produces control actions equal to

$$u(t) = P\left(e(t) + \frac{1}{I}\int_0^t e(\tau)\mathrm{d}\tau + D\frac{\mathrm{d}e(t)}{\mathrm{d}t}\right), \tag{3.5}$$

where P is the proportional gain, I the integral time constant, D the derivative time constant and $e(t)$ is an error between a measured process variable and its desired value. Functionality of respective terms can be described as follows

- The proportional term – providing an overall control action proportional to the error signal through the all-pass gain factor.
- The integral term – reducing steady-state errors through low-frequency compensation by an integrator.

- The derivative term – improving transient response through high-frequency compensation by a differentiator.

Thus, through the integral and derivative term, the PID regulator can be understood as a controller that takes also the past and future errors into consideration.

For the optimum performance of the regulator, parameters P, I, and D have to be set properly. Nonetheless, it is generally impossible to outline optimal values for parameters theoretically. Due to this fact, they are obviously tuned manually or by some adaptive method, see e.g. [1]. More extensive introduction into the PID regulator problematics can be found in [17].

It should be pointed out that the relation between the PID regulator and the original problem is only through the parameters P, I, and D. As a consequence, it is hard to say how to change the parameters when the parameters of the system are changed. This hidden relation makes a detailed study of the regulator practically impossible.

If a system controlled by the PID regulator is in a fixed state which match with desired state, all the terms in (3.5) will be zero and thus also the proposed control actions will be zero. If the system state is known exactly, it is certainly the best controlling. Nevertheless, in the control problem under uncertainty, we have only some approximation of the true state, e.g. its mean value, which is controlled by the PID regulator and the PID regulator does not provide active probing which would causes better identification of the system. As consequence, the PID regulator is not dual controller.

3.4 Cautious control and Certainty equivalence principle

Cautious control and Certainty equivalence principle are commonly used approaches for simplification of the original problem (3.3), see [3].

Cautious Control (CC) is obtained by a restriction of the original optimization problem to a horizon of length $N = 1$. The name origins from the fact that the optimization of control actions does not incorporate the advantage of probing. The simplification by certainty equivalence principle replaces all the random variables in (3.3) by their mean values, this gives Certainty Equivalence Control (CEC). Of course, both approaches can be combined.

Both approximation techniques provide a control policy which is not dual, however these techniques are often the only ones which are able to propose control policy based on original problem and which allows online computations.

3.5 Methods based on stochastic approximations

Mayor advantage of methods based on stochastic approximation of the original problem is their generality. However, based on author's knowledge, there is no method of this kind which overcomes the so called curse of dimenzionality – the fact that complexity of the problem increases exponentially in higher dimensions, longer horizon of simulation or more dense of approximation.

3.5.1 Stochastic iterative approximations of dynamic programming (SIDP)

Method of Stochastic iterative Approximations of Dynamic programming (SIDP) was proposed in [27]. It is based on two main principles:

- solving the dynamic programming (3.3) in several iterations rather than in only one step,
- using Monte Carlo approximation of expectations in (3.3).

The first approach is so called Iterative Dynamic Programming (IDP). In [27], it was shown that under relatively general assumptions, control policy iterations provided by the SIDP algorithm converges to the optimal policy regardless of the initial policy. Moreover using IDP, it is sufficient to use less points in discretization of the space because only the part of the space which could be reached in current iteration has to be discretized.

The algorithm proceeds offline and provides the control policy in a form of control actions for every discretized point and every time step. Then, controlling is performed using these prepared control actions. In the original article, the control actions outside the discretized points are linearly interpolated.

However, SIDP algorithm has exponential computational complexity in horizon length and thus can be applied on systems with long transient response only with huge computational effort, see [27] for evidence. Moreover, if the system noise is relatively large, convergence of the algorithm is very slow or even unstable.

3.5.2 Stochastic approximations of policy gradient

Stochastic approximations of policy gradient was presented in [26], here is also the proof of optimality of the algorithm. Principally, the computation of optimal control action uses stochastic approximations of the gradient of (3.2) with respect to the control actions $u_{0:N-1}$ and then the gradient descent algorithm is utilized for finding the optimum.

In the original article [26], Open-Loop Feedback Control (OLFC) approach is used. The approach lies in optimizing the (3.2) at horizon $t = k, \ldots, N$ during every time

step k, see [3]. The disadvantage of OLFC approach is that it is inapplicable on real-time applications because the computation of single step of the algorithm is relatively time consuming.

Chapter 4

Simulations

In this chapter, the application of previously presented estimating and controlling techniques on a real model is presented.

4.1 Model of permanent magnet synchronous machine drive

We will be interested in model of Permanent Magnet Synchronous Machine drive with surface magnets on the rotor (abbreviated as PMSM). Following description is adopted from [22].

4.1.1 Time continuous model

The model is described by conventional equations in a stationary reference frame

$$\frac{\mathrm{d}i_\alpha}{\mathrm{d}t} = -\frac{R}{L}i_\alpha + \frac{\Psi}{L}\omega\sin\theta + \frac{u_\alpha}{L} \tag{4.1}$$

$$\frac{\mathrm{d}i_\alpha}{\mathrm{d}t} = -\frac{R}{L}i_\beta - \frac{\Psi}{L}\omega\cos\theta + \frac{u_\beta}{L} \tag{4.2}$$

$$\frac{\mathrm{d}\omega}{\mathrm{d}t} = \frac{k_p p_p^2 \Psi}{J}(i_\beta\cos\theta - i_\alpha\sin\theta) - \frac{B}{J}\omega - \frac{p_p}{J}T \tag{4.3}$$

$$\frac{\mathrm{d}\theta}{\mathrm{d}t} = \omega. \tag{4.4}$$

Here, i_α, i_β, u_α and u_β represent stator currents and voltages in the stationary reference frame, respectively; ω is electrical rotor speed and θ is electrical rotor position. R and L is stator resistance and inductance respectively, Ψ is the flux of permanent magnets on the rotor, B is friction and T is load torque, J is moment of inertia, p_p is the number of pole pairs, k_p is the Park constant.

The goal is to design a control policy for voltages which will result into the desired

original term	substitution	value in simulations
$1 - \frac{R}{L}\Delta t$	a	0.9898
$\frac{\Psi}{L}\Delta t$	b	0.0072
$\frac{\Delta t}{L}$	c	0.0361
$1 - \frac{B}{J}\Delta t$	d	1
$\frac{k_p p_p^2 \Psi}{J}\Delta t$	e	0.0149

Table 4.1: Parameters of the PMSM.

rotor speed $\bar{\omega}$. The loss function is quadratic

$$\int_0^T v(u_\alpha^2(t) + u_\beta^2(t)) + (\omega(t) - \bar{\omega}(t))^2 \mathrm{d}t, \tag{4.5}$$

where v is some known constant. During simulations, we use $v = 0.1$. We also consider a constraint on voltages in the form

$$\sqrt{u_\alpha^2 + u_\beta^2} \leq 100. \tag{4.6}$$

4.1.2 Discretized model

Discretization of the model was performed using Euler method with the following result:

$$i_{\alpha,t+1} = (1 - \frac{R}{L}\Delta t) i_{\alpha,t} + \frac{\Psi}{L}\Delta t \omega_t \sin\theta_t + \frac{\Delta t}{L} u_{\alpha,t} \tag{4.7}$$

$$i_{\beta,t+1} = (1 - \frac{R}{L}\Delta t) i_{\beta,t} - \frac{\Psi}{L}\Delta t \omega_t \cos\theta_t + \frac{\Delta t}{L} u_{\beta,t} \tag{4.8}$$

$$\omega_{t+1} = (1 - \frac{B}{J}\Delta t)\omega_t + \Delta t \frac{k_p p_p^2 \Psi}{J}(i_{\beta,t}\cos\theta_t - i_{\alpha,t}\sin\theta, t) - \frac{p_p}{J} T \Delta t \tag{4.9}$$

$$\theta_{t+1} = \theta_t + \omega_t \Delta t. \tag{4.10}$$

For simplifying the notation, we make a substitution summarized in table 4.1 (we consider parameters of the model known). It results in

$$i_{\alpha,t+1} = a i_{\alpha,t} + b\omega_t \sin\theta_t + c u_{\alpha,t} \tag{4.11}$$

$$i_{\beta,t+1} = a i_{\beta,t} - b\omega_t \cos\theta_t + c u_{\beta,t} \tag{4.12}$$

$$\omega_{t+1} = d\omega_t + e(i_{\beta,t}\cos\theta_t - i_{\alpha,t}\sin\theta_t) \tag{4.13}$$

$$\theta_{t+1} = \theta_t + \omega_t \Delta t. \tag{4.14}$$

The state variables and the voltages can be aggregated into $x_t = (i_{\alpha,t}, i_{\beta,t}, \omega_t, \theta_t)^T$ and $u_t = (u_{\alpha,t}, u_{\beta,t})^T$. The constraint on u_t is then

$$||u_t|| \leq 100. \tag{4.15}$$

Discretized loss function is of the form

$$\sum_0^N u_t^T \Gamma u_t + (x_t - \bar{x}_t)^T \Xi (x_t - \bar{x}_t), \tag{4.16}$$

where we denoted

$$\Gamma = \begin{pmatrix} v & 0 \\ 0 & v \end{pmatrix}, \qquad \Xi = \begin{pmatrix} 0 & 0 & 0 & 0 \\ 0 & 0 & 0 & 0 \\ 0 & 0 & 1 & 0 \\ 0 & 0 & 0 & 0 \end{pmatrix}. \tag{4.17}$$

The sensor-less control scenario arise when sensors of the speed and position are missing (from various reasons). The only observable variables are thus $(i_{\alpha,t}, i_{\beta,t})$, however, only up to some precision. In relation to the chapter 1, the system is modeled as Markovian state-space model given by

$$x_t = g(x_{t-1}, u_{t-1}) + w_{t-1} \qquad t \geq 0, \tag{4.18}$$

$$y_t = Hx_t + v_t, \tag{4.19}$$

where $H = \begin{pmatrix} 1 & 0 & 0 & 0 \\ 0 & 1 & 0 & 0 \end{pmatrix}$, $w_{t-1} \sim \mathcal{N}(0, Q)$ and $v_t \sim \mathcal{N}(0, R)$. In later simulations, we use

$$Q = \mathrm{diag}(0.0013, 0.0013, 5 \times 10^{-6}, 10^{-10}), \tag{4.20}$$

$$R = \mathrm{diag}(0.0006, 0.0006). \tag{4.21}$$

Values for matrices Q and R and parameters in table 4.1 are adopted from [22], where real prototype of the PMSM was analyzed.

4.2 Application of presented estimating techniques on the PMSM

In this section, estimating techniques described in chapter 2 are applied on the PMSM.

4.2.1 Particle filters

As was mentioned in section 2.4, the importance density which minimizes the variance of the importance weight is $p(x_t|x_{t-1}, y_t)$ and particular case of Gaussian state space model with non-linear system equation allows analytic solution. Following results are adopted from [7]. Defining

$$S^{-1} = Q^{-1} + H^T R H, \tag{4.22}$$

$$m_t = S(Q^{-1} g(x_{t-1}) H^T R y_t), \tag{4.23}$$

one can obtain

$$x_t|(x_{t-1}, y_t) \sim \mathcal{N}(m_t, S), \tag{4.24}$$

and

$$p(y_t|x_{t-1}) \propto exp\left(-\frac{1}{2}(y_t - Hg(x_{t-1}))^T (R + HQH^T)^{-1}(y_t - Hg(x_{t-1}))\right). \tag{4.25}$$

We denote $\mathrm{SIR}_{\mathrm{opt}}$ a version of the SIR filter with the optimal importance density. For later comparison, we also denote $\mathrm{SIR}_{\mathrm{prior}}$ a version of the SIR filter in which the prior density as the importance density is used.

Although particle filters can be theoretically used for arbitrary large state space, estimation in multidimensional states is less accurate because of need of larger amount of particles for sufficient coverage of the space. For reducing the amount of particles needed for efficient approximation of the space, we use estimation by a particle filter only in unobservable (ω_t, θ_t); as estimator for $(i_{\alpha,t}, i_{\beta,t})$, we use only observed values. In other words, we consider only two dimensional state space with ω_t and θ_t It incorporates errors caused by noisy observations, however, nearly the same level of accuracy can be achieved by usage of significantly less particles than in the case of full four dimenzional state space (about 25x lesser).

We also tested the ASIR filter, nonetheless, similar state space reduction as before is not functioning well. It is due to the fact, that usage of only single point for approximation of currents increases noises and as was mentioned in [2] in the case of too noisy observations the performance of the ASIR filter is unreliable. Consequently, inside the ASIR filer, the whole state x_t is approximated by particles.

Using both the $\mathrm{SIR}_{\mathrm{prior}}$ and ASIR filter, performance using true matrix R was insufficient; both filters was too restrictive during weight updating step and often converge to a wrong state. Overall performance was improved by using covariance matrix $\tilde{R} = \rho R$ instead of R, where $\rho > 1$ is a real parameter. An amplification of ρ increases the robustness of the respective particle filter but in a case of convergence it also increases the average error of estimation. Proper ρ should be chosen after some initial simulations. Based on several quantitative test, we will use $\rho = 100$ in case of $\mathrm{SIR}_{\mathrm{prior}}$ and even $\rho = 1000$ for the ASIR filter. Moreover, we found that the failure of estimation also occurs in case where $\mathrm{SIR}_{\mathrm{opt}}$ is used but the number of failures were much more lesser than in cases of the $\mathrm{SIR}_{\mathrm{prior}}$ and ASIR filter. Nonetheless, we will incorporate the same approach to add robustness by using $\rho = 10$.

Moreover, we found that the number of particles can be lowered (approximately 5x) without a loss of accuracy if larger variance on θ is used. Thus in all particle filters, we use $\tilde{\sigma}_\theta^2 = 10^{-4}$ instead of true $\sigma_\theta^2 = 10^{-10}$.

Using small number of particles, it may happen that the estimation process is corrupted when particles approximating the initial state are generated very unevenly. For overcoming this problem, particles approximating initial distribution are chosen equidistantly in interval $[-\pi, \pi]$ instead of random samples.

Performance using different resampling procedures was nearly the same in our simulations, thus, we use only deterministic resampling for its computational effectiveness and fully deterministic version of residual resampling in cases when we would like to omit effects caused by random realizations inside a particle filter.

In later simulations, we want to be able to estimate θ wherever can be in interval $(-\pi, \pi)$. As consequence, if we have no additional initial information, we have to have whole the interval $(-\pi, \pi)$ discretized in the initial distribution on θ. This may cause a problem when the true state is close to one of the boundary values – large

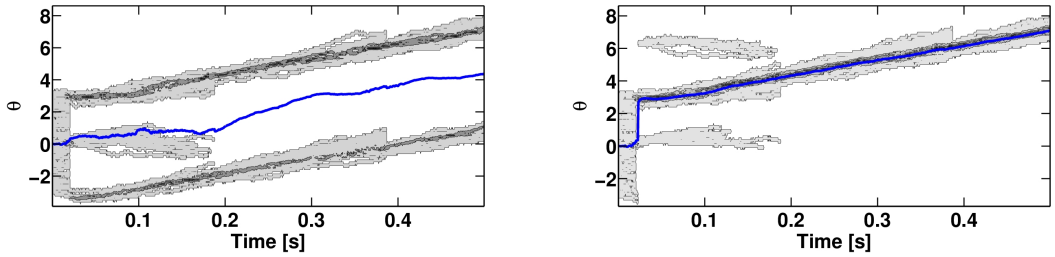

Figure 4.1: The figure shows a probabilistic distribution in respective times (darker color means higher probability) and mean values of the distributions. In the right figure, the transformation (4.26) is incorporated.

weight will obtain both particles with θ close to $-\pi$ and π because of periodicity of trigonometric functions. It may degrade estimations based on this approximation, in extreme case for example $\cos\mathrm{E}\{\theta\} \approx -1$, although $\mathrm{E}\{\cos\theta\} \approx 1$. This particular problem makes CEC regulator unable to reach the desired state when the initial state is close to π (or $-\pi$). This can be overcame by utilizing not the $\cos\mathrm{E}\{\theta\}$ but $\mathrm{E}\{\cos\theta\}$. Another (and also more general) possibility how to overcome the problem is to make the approximation on θ continuous in π when it is useful. It can be done by transformation

$$\Phi(\theta) = \begin{cases} \theta & \text{if } \theta > 0, \\ \theta + 2\pi & \text{otherwise.} \end{cases} \tag{4.26}$$

The transformation overcomes the discontinuity in π. As a suitable indicator for introducing the transformation, we utilize the standard deviation of estimates based on distributions before and after the transformation (denoted σ_1 and σ_2). If $\sigma_1 \geq 1.5\sigma_2$, we utilize the transformation. Practical usage of the transformation is shown in figure 4.2.1

4.2.2 EKF

By linearization of the model in $\hat{x}$, and using notation from section 2.8, we obtain (note, that the equation for observation is already linear)

$$A_t = \begin{pmatrix} a & 0 & b\,\sin\hat{\theta}_t & b\hat{\omega}_t\,\cos\hat{\theta}_t \\ 0 & a & -b\,\cos\hat{\theta}_t & b\hat{\omega}_t\,\sin\hat{\theta}_t \\ -e\,\sin\hat{\theta}_t & e\,\cos\hat{\theta}_t & d & -e(\hat{i}_{\beta,t}\,\sin\hat{\theta}_t + \hat{i}_{\alpha,t}\,\cos\hat{\theta}_t) \\ 0 & 0 & \Delta t & 1 \end{pmatrix}. \tag{4.27}$$

Having an initial distribution $x_0 \sim \mathcal{N}(\hat{x}_{0|0}, P_{0|0})$, computation of the EKF can proceed directly using equations from section 2.8.

As will be shown in subsection 4.4.2, the EKF is unable to filter proposed density properly in cases where only a weak prior information is available. However, as is generally known (e.g [5]), performance of the EKF can be improved by using some matrices $\tilde{Q}$ and $\tilde{R}$ during estimation step instead of original matrices Q and R. Estimation with matrices containing greater diagonal elements is more sensitive on differences between predicted and observed values and thus the estimation

is less conservative, although proposed estimates are still only Gaussian distributions. These properties was observed also in our simulations, however, no settings of the matrices resulted into a sufficient reliability. This issue is shortly discussed in respective subsection.

4.3 Application of presented controling techniques on the PMSM

In this section, an implementation of the PID, CC and CEC regulator is presented. A control policy proposed by the SIDP algorithm (or extensions of previous controlling techniques enhanced by the SIDP) does not work well, so we omit details of its implementation on the PMSM. The algorithm of stochastic policy gradient was not implemented because, due to the mentioned computational complexity, it is improper for application on the PMSM.

4.3.1 PI regulator

Historically, first PID regulators consisted from only of two components – the proportional one and the integral one. The derivative term was added to stabilize the system against overshoots caused by the integral component. However, the derivative term slows transient response and causes instability of the PID regulator if noises are sufficiently large, see [1]. Due to this fact and the fact that the transient response of the PMSM is also very large (affected by small Δt), we omit the derivative term in our implementation of the PID regulator on the PMSM.

The classical PI regulator control is based on transformation to $d-q$ reference frame (for detailed derivation see [28])

$$i_d = i_\alpha \cos(\theta) + i_\beta \sin(\theta), \tag{4.28}$$
$$i_q = i_\beta \cos(\theta) - i_\alpha \sin(\theta). \tag{4.29}$$

For desired ω, firstly, we compute target i_q current, denoted $\bar{i}_q$. It is derived using the PI regulator

$$\bar{i}_q = \mathrm{PI}(\bar{\omega} - \omega, P_i, I_i), \tag{4.30}$$

where an arbitrary PI controller is defined as follows

$$x = \mathrm{PI}(\epsilon, P, I) = P\epsilon + I(S_{t-1} + \epsilon), \tag{4.31}$$
$$S_t = S_{t-1} + \epsilon. \tag{4.32}$$

This current needs to be achieved through voltages u_d, u_q which are again obtained from PI regulators

$$u_d = \mathrm{PI}(-i_d, P_u, I_u), \tag{4.33}$$
$$u_q = \mathrm{PI}(\bar{i}_q - i_q, P_u, I_u). \tag{4.34}$$

Because of a magnetic field caused by the rotor motion, voltages are compensated by

$$u_d = u_d - L_s \omega \bar{i}_q, \tag{4.35}$$
$$u_q = u_q + \Psi_{pm} \omega. \tag{4.36}$$

Conversion to u_α, u_β is done by

$$u_\alpha = |U| \cos\phi, \tag{4.37}$$
$$u_\beta = |U| \sin\phi, \tag{4.38}$$

where

$$|U| = \sqrt{u_d^2 + u_q^2} \qquad \phi = \begin{cases} \arctan\frac{u_d}{u_q} + \theta & \text{if } u_d \geq 0, \\ \arctan\frac{u_d}{u_q} + \theta + \pi & \text{if } u_d < 0. \end{cases} \tag{4.39}$$

In order to satisfy the constraint (4.15), if $U > 10$, we firstly set $U := 10$.

Based on several initial simulations, constants for PI regulators were set on

$$P_i = 3, \qquad I_i = 0.00375, \tag{4.40}$$
$$P_u = 20, \qquad I_u = 0.5. \tag{4.41}$$

It should be noted that the PI regulator is based on the value of the true state . Having only an estimate of the state, we are tended to use some characteristic of probability distribution of the state, for example mean value. Another possibility could be maximum value or random sample from the distribution, however, these are more sensitive on accuracy of the estimate and, in a case of large uncertainty, they often propose unstable control actions. Due to this, we will aim only on the PI regulator computed for mean value.

4.3.2 Cautious control

Because an arbitrary input of u_t can cause any changes firstly in ω_{t+2}, we derive the cautious control by minimization of

$$u_t^T \Gamma u_t + \mathrm{E}\big((x_{t+1} - \bar{x}_{t+1})^T \Xi (x_{t+1} - \bar{x}_{t+1}) + (x_{t+2} - \bar{x}_{t+2})^T \Xi (x_{t+2} - \bar{x}_{t+2})\big). \tag{4.42}$$

We note that the first term in the expectation can be omitted due to the fact that its derivative with respect to u_t is zero, however, we keep it for better readability in a later text.

We outline only an unconstrained minimization of (4.42). If obtained control action u_t does not satisfy the constraint (4.15), we define

$$u_t := 10 \frac{u_t}{||u_t||}. \tag{4.43}$$

The unconstrained minimization can be performed by setting first derivative of (4.42) with respect to u_t to zero, thus using the symmetry of Γ and Ξ

$$u_t^T \Gamma + \mathrm{E}\left((x_{t+1} - \bar{x}_{t+1})^T \Xi \frac{\partial x_{t+1}}{\partial u_t} + (x_{t+2} - \bar{x}_{t+2})^T \Xi \frac{\partial x_{t+2}}{\partial u_t}\right) = 0. \tag{4.44}$$

Due to that the control action at $t+1$ does not affect any change in ω, x_{t+2} can be expressed as

$$x_{t+1} = A_t x_t + C u_t + w_t \tag{4.45}$$
$$x_{t+2} = A_{t+1} x_{t+1} + w_{t+1} = A_{t+1} A_t x_t + A_{t+1} C u_t + A_{t+1} w_t + w_{t+1}, \tag{4.46}$$

where A_t and C are

$$A_t = A(x_t) = \begin{pmatrix} a & 0 & b\,\sin\theta_t & 0 \\ 0 & a & -b\,\cos\theta_t & 0 \\ -e\,\sin\theta_t & e\,\cos\theta_t & d & 0 \\ 0 & 0 & \Delta t & 1 \end{pmatrix}, \qquad C = \begin{pmatrix} c & 0 \\ 0 & c \\ 0 & 0 \\ 0 & 0 \end{pmatrix}. \tag{4.47}$$

It should be mentioned, that although system equation (4.46) is expressed only using linear operations, it does not mean that the system is linear because matrix A_t is a nonlinear function of x_t.

After the substitution in (4.42) and a small simplification, we obtain

$$\begin{aligned} u_t^T \Gamma + \mathrm{E}\big((A_t x_t - \bar{x}_{t+1})^T \Xi + (A_{t+1} A_t x_t - \bar{x}_{t+2})^T \Xi A_{t+1}\big) C + \\ + u_t^T C^T \mathrm{E}\left(\Xi + A_{t+1}^T \Xi A_{t+1}\right) C = 0. \end{aligned} \tag{4.48}$$

Denoting

$$\Lambda_2 = \mathrm{E}\big((A_t x_t - \bar{x}_{t+1})^T \Xi + (A_{t+1} A_t x_t - \bar{x}_{t+2})^T \Xi A_{t+1}\big) C, \tag{4.49}$$
$$\Sigma_2 = C^T \mathrm{E}\left(\Xi + A_{t+1}^T \Xi A_{t+1}\right) C, \tag{4.50}$$

we have CC action u_t in a form

$$u_t^T = \Lambda_2 (\Gamma + \Sigma_2)^{-1}. \tag{4.51}$$

Nonetheless, the proposed control policy will not work properly. It is due to the fact, that matrix Λ_2 has elements multiplied by $ce \approx 5.10^{-4}$ meanwhile dominant elements of the matrix in denominator are close to $v = 0.1$. Then, the proposed control action u_t will be close to zero as can be viewed clearly from the following example. Suppose $i_{\alpha,t}, i_\beta, \omega_t$ known and equal to zero and $\bar{\omega}_{t+2} = 10\mathrm{rad.s}^{-1}$. Under this assumption, the norm of the proposed control action is bounded by

$$||u_t||^2 = u_t^T u_t \leq \left(\frac{10ce}{v}\right)^2 \mathrm{E}\left\{\begin{pmatrix} \sin\theta_t \\ \cos\theta_t \end{pmatrix}^T\right\} \mathrm{E}\left\{\begin{pmatrix} \sin\theta_t \\ \cos\theta_t \end{pmatrix}\right\} < 5.10^{-4}\,. \tag{4.52}$$

There are several possibilities how to overcome this. The most straightforward possibility is to artificially decrease v when u_t is computed. Based on experiments which are not included, decrease of v under 10^{-4} yields into a control policy which is able to reach desired $\bar{\omega}_t$. However, this solution of the problem is improper because the control policy does not take into consideration future effects of u_t. This policy often overshoot the desired value of the velocity and results into damped oscillations.

A more natural way for overcoming the problem of too small control actions obtained from (4.51) is to incorporate effects of u_t at a longer horizon. For arbitrary $k \in \mathbb{N}$, we can extend the loss (4.42) by future losses and to write

$$J = u^T \Gamma u_t + \mathrm{E}\left(\sum_{k=1}^{n} (x_{t+k} - \bar{x}_{t+k})^T \Xi (x_{t+k} - \bar{x}_{t+k})\right). \tag{4.53}$$

Similarly as before, future states can be evaluated as

$$x_{t+1} = A_t x_t + C u_t + w_t \tag{4.54}$$

$$\begin{aligned} x_{t+k} &= A_{t+k-1} x_{t+k-1} + w_{t+k-1} = \\ &= A_{t+k-1} A_{t+k-2} x_{t+k-2} + A_{t+k-1} w_{t+k-2} + w_{t+k-1} = \ldots = \\ &= \left(\prod_{l=0}^{k-1} A_{t+l}\right) x_t + \left(\prod_{l=1}^{k-1} A_{t+l}\right) C u_t + \sum_{l=0}^{k-1} \left(\left(\prod_{m=l+1}^{k-1} A_{t+m}\right) w_{t+l}\right), \end{aligned} \tag{4.55}$$

where the products have to be understood by matrix multiplications in correct order.

After simplification, the condition for unconstrained minimization have the form

$$\begin{aligned} u_t^T \Gamma + \mathrm{E}\left\{\sum_{k=1}^{n} \left(\left(\left(\prod_{l=0}^{k-1} A_{t+l}\right) x_t - \bar{x}_{t+k}\right)^T \Xi \left(\prod_{l=1}^{k-1} A_{t+l}\right)\right)\right\} C + \\ + u_t^T C^T \mathrm{E}\left\{\sum_{k=1}^{n} \left(\left(\prod_{l=1}^{k-1} A_{t+l}\right)^T \Xi \left(\prod_{l=1}^{k-1} A_{t+l}\right)\right)\right\} C = 0. \end{aligned} \tag{4.56}$$

Thus, we can use previous notation denoting

$$\Lambda_n = \mathrm{E}\left\{\sum_{k=1}^{n} \left(\left(\left(\prod_{l=0}^{k-1} A_{t+l}\right) x_t - \bar{x}_{t+k}\right)^T \Xi \left(\prod_{l=1}^{k-1} A_{t+l}\right)\right)\right\} C, \tag{4.57}$$

$$\Sigma_n = C^T \mathrm{E}\left\{\sum_{k=1}^{n} \left(\left(\prod_{l=1}^{k-1} A_{t+l}\right)^T \Xi \left(\prod_{l=1}^{k-1} A_{t+l}\right)\right)\right\} C, \tag{4.58}$$

and to obtain CC action as

$$u_t^T = \Lambda_n (\Gamma + \Sigma_n)^{-1}. \tag{4.59}$$

Computation of Λ_n and Σ_n is relatively time consuming and for n for which the proposed control law could be sufficient, the online computation is impossible. Nonetheless, the computation can be greatly speed up by the following approximation. Let n is sufficiently small that $\{\theta_{t+k}\}_{k=0}^{n}$ is a constant sequence up to some desired level and effects of the magnetic induction in equations for the currents can be neglected. In other words, we use an approximation

$$A_t \approx A_{t+l} \approx \tilde{A} = \begin{pmatrix} a & 0 & 0 & 0 \\ 0 & a & 0 & 0 \\ -e\,\sin\theta_t & e\,\cos\theta_t & d & 0 \\ 0 & 0 & 0 & 1 \end{pmatrix} \qquad l = 0, \ldots, n \tag{4.60}$$

Due to this approximation, we can express

$$\prod_{l=0}^{k-1} A_{t+l} \approx \tilde{A}^k = \begin{pmatrix} a^k & 0 & 0 & 0 \\ 0 & a^k & 0 & 0 \\ -eS_k \sin\theta_t & eS_k \cos\theta_t & d^k & 0 \\ 0 & 0 & 0 & 1 \end{pmatrix}, \tag{4.61}$$

where

$$S_k = \sum_{l=0}^{k-1} a^l d^{k-1-l} = d^{k-1} \sum_{l=0}^{k-1} \left(\frac{a}{d}\right)^l = \frac{d^k - a^k}{d-a}. \tag{4.62}$$

After simplification, we obtain Λ_n and Σ_n approximated as

$$\begin{aligned} \Lambda_n \approx{}& \gamma_n \mathrm{E}\left\{ \begin{pmatrix} i_{\alpha,t} \\ i_{\beta,t} \end{pmatrix}^T \begin{pmatrix} \sin^2\theta_t & -\sin\theta_t\cos\theta_t \\ -\sin\theta_t\cos\theta_t & \cos^2\theta_t \end{pmatrix} \right\} + \\ &+ \sum_{k=1}^{n} \left(ceS_{k-1} \left(d^k \mathrm{E}\left\{ \omega_t \begin{pmatrix} \sin\theta_t \\ \cos\theta_t \end{pmatrix}^T \right\} - \bar{\omega}_{t+k} \mathrm{E}\left\{ \begin{pmatrix} \sin\theta_t \\ \cos\theta_t \end{pmatrix}^T \right\} \right) \right) \end{aligned} \tag{4.63}$$

$$\Sigma_n \approx \delta_n \mathrm{E}\left\{ \begin{pmatrix} \sin^2\theta_t & -\sin\theta_t\cos\theta_t \\ -\sin\theta_t\cos\theta_t & \cos^2\theta_t \end{pmatrix} \right\}, \tag{4.64}$$

where for $d \neq 1$ (for $d = 1$ is the computation even simpler)

$$\begin{aligned} \gamma_n &= ce^2 \sum_{k=1}^{n} S_k S_{k-1} = c\left(\frac{e}{d-a}\right)^2 \sum_{k=0}^{n-1} \left(d(d^2)^k - (a+d)(ad)^k + (a^2)^k \right) = \\ &= c\left(\frac{e}{d-a}\right)^2 \left(d\frac{1-d^{2n}}{1-d^2} - (a+d)\frac{1-(ad)^n}{1-ad} + a\frac{1-a^{2n}}{1-a^2} \right), \end{aligned} \tag{4.65}$$

$$\begin{aligned} \delta_n &= c^2e^2 \sum_{k=1}^{n} S_{k-1}^2 = \left(\frac{ce}{d-a}\right)^2 \sum_{k=0}^{n-1} ((d^2)^k - 2(ad)^k + (a^2)^k) = \\ &= \left(\frac{ce}{d-a}\right)^2 \left(\frac{1-d^{2n}}{1-d^2} - 2\frac{1-(ad)^n}{1-ad} + \frac{1-a^{2n}}{1-a^2} \right). \end{aligned} \tag{4.66}$$

For comparison with the case without incorporating the future loss, we consider similar example as before in (4.52). For $\bar{\omega}_{t+k} = 10\mathrm{rad.s}^{-1}$ for $k = 1, \ldots, n$, we obtain an estimate

$$||u_t||^2 = u_t^T u_t \approx \left(\frac{10ce}{v} \sum_{k=1}^{n} S_{k-1} \right)^2 \mathrm{E}\left\{ \begin{pmatrix} \sin\theta_t \\ \cos\theta_t \end{pmatrix}^T \right\} \mathrm{E}\left\{ \begin{pmatrix} \sin\theta_t \\ \cos\theta_t \end{pmatrix} \right\}. \tag{4.67}$$

This expression gives an intuitive recipe for appropriate n. A successful policy is obtained by choice $n \geq 50$. In later simulations we use $n = 80$, what corresponds to incorporating the loss generated in horizon $t = 0.01\mathrm{s}$. However, the quality of the control is only a little sensitive and control actions are nearly the same for a large range of n.

Approximation of (4.59) by (4.63) and (4.64) can be computed very efficiently. Expectations can be approximated by estimates proposed by a particle filter. Furthermore, constants γ_n and δ_n can be computed offline.

More crucial problem with the control policy generated according to (4.59) is its caution. To illustrate this, suppose, that $i_{\alpha,t}, i_\beta$ is known and equal to zero, ω_t is independent on θ and $\theta \sim \mathrm{U}(-\pi, \pi)$. This assumption holds for example for $t = 0$ if we have no additional initial information. From (4.63) or (4.67), we can see that the norm of the proposed control action will be zero regardless on differences between the actual and the desired state.

4.3.3 Certainty equivalence control

The problem from the end of subsection 4.3.2 can be dealt by utilizing the principle of Certainty Equivalence Control (CEC). According to that, we replace all the random variables in (4.63) and (4.64) by their mean values.

4.3.4 Dual control

Another possibility how to overcome the excessive caution of CC regulator is to add some probing term according to (3.4). At first, we denote

$$\alpha(x_t) = \left|\left| \mathrm{E}\left\{ \begin{pmatrix} \sin\theta_t \\ \cos\theta_t \end{pmatrix} \right\} \right|\right|_2 . \tag{4.68}$$

Because $0 \leq \alpha(x_t) \geq 1$, where the lower bound is reached for uniform distribution and the upper bound for Dirac distribution, $\alpha(x_t)$ is proper measure for introducing some probing term. As a consequence, we modify the original CC regulator as follows

$$u_t = \alpha(x_t)\mathrm{CC}(x_t) + (1 - \alpha(x_t))u_t^{\mathrm{prob}}, \tag{4.69}$$

where $\mathrm{CC}(x_t)$ is control action computed by (4.59) and u_t^{prob} is some probing term.

Based on our experience with the system, reasonable choice of probing term is generator of constant voltage whose phase is changing monotonically

$$u_t^{\mathrm{prob}} = U_0 \begin{pmatrix} \sin\left(\frac{2\pi}{T}t + \phi_0\right) \\ \cos\left(\frac{2\pi}{T}t + \phi_0\right) \end{pmatrix}. \tag{4.70}$$

Parameters of the probing term has to be tuned, we utilize $U_0 = 10$, $T = 240$ (corresponds to turning by 2π every 0.06s) and $\phi_0 = 0$. Although here is necessity of tuning the regulator, every parameter has simple meaning and proper setting can be done intuitively after few initial simulations.

4.3.5 SIDP

The SIDP algorithm was implemented and tested without obtaining any sufficient results. The algorithm was also implemented for improving previously presented reg-

ulators by perturbations, however, again with no measurable improvements. Based on author's opinion, it is due to the fact, that the optimization in (3.3) is performed step by step, although due to the long transient response and relatively large noise, a profit from only one single control action is hard to evaluate. A successful control policy should give similar control action for sufficiently long horizon to cause any measurable effects and, as a consequence, to improve the identification and to allow better control in future. To obtain this behavior by optimizing step by step, it would take a large amount of iterations of the algorithm.

Nonetheless in contrary to the original PI, CC and CEC regulator, the SIDP algorithm could provide control actions which would have the dual character naturally. This attractive property could motivate develop of some modifications of SIDP.

4.4 Results

4.4.1 Test scenario

The most challenging problem with the PMSM is starting phase without any initial information on θ. Difficulties arise due to the symmetry of the system and long delays between actions and measurable responses. The performance of particle filters and the EKF is compared.

The goal is to linearly increase the velocity during 0.1s from 0 up to 10rad.s^{-1} and to keep this value for next 0.1s. The initial state is drawn randomly from distribution representing the initial estimate.

$$\begin{aligned} i_{\alpha,0} &\sim \mathcal{U}(-0.01, 0.01) \\ i_{\alpha,0} &\sim \mathcal{U}(-0.01, 0.01) \\ \omega &\sim \mathcal{U}(-0.01, 0.01) \\ \theta &\sim \mathcal{U}(-\pi, \pi). \end{aligned} \tag{4.71}$$

4.4.2 Qualitative comparison of filters

In this subsection, the qualitative results of estimating by $\mathrm{SIR}_{\mathrm{opt}}$ filter and the EKF are presented. Results for the ASIR filter and the $\mathrm{SIR}_{\mathrm{prior}}$ filter are omitted because are (qualitatively) near the same. Comparison of these variants of a particle filter is included in subsection 4.4.4.

For the $\mathrm{SIR}_{\mathrm{opt}}$ filter, we use $N = 60$, $N_{thresh} = N/5 = 12$ and deterministic resampling procedure. Control actions are generated by the PI regulator for mean value of estimated distribution.

Results of one realization are summarized in figure 4.4.2. In contrast to the $\mathrm{SIR}_{\mathrm{opt}}$ filter, controlling based on the EKF produces only small control actions. It is due to the fact, that mean value of the estimate proposed by the EKF match with the desired state well and, thus, only small control actions are necessary. However, small

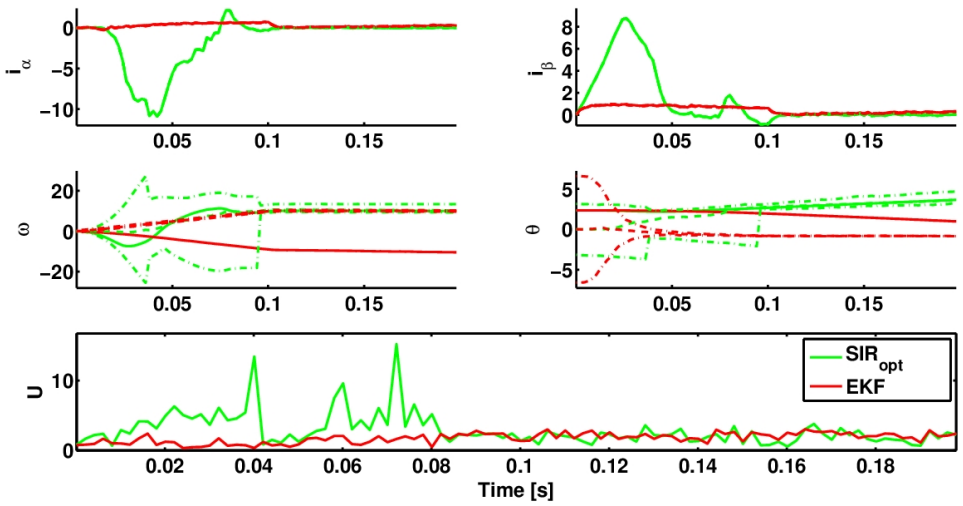

Figure 4.2: Qualitative comparison of different filters. For ω_t and θ_t, the true state is marked by the full line, the estimate by the dashed line, and bound of the estimated distribution (in case of the SIR_{opt}) and the variance (in case of the KF) by the dash-dot line.

actions are not very informative which cause failure of the EKF. As consequence of the failure, the EKF convergences to the state with angle shifted by π from the true state. It causes turning in opposite direction. On the other hand, in cases where better initial information is available (and thus better performance of the EKF is assumed), the EKF would be able to reach desired state very effectively. Another remarkable result is that the highest voltages are reached just after resampling procedure is utilized (sharp edges in the estimates of posterior distribution). Similarly, the highest currents are reached just after estimates proposed by the SIR_{opt} filter become sufficiently accurate.

The wrong convergence of the EKF is caused by the assumption that the posterior distribution can be sufficiently approximated by Gaussian distribution. Nevertheless, the estimated posterior distribution proposed by the SIR_{opt} filter shows that the assumption is improper (at least during first 0.1s), see figures 4.3 and 4.4. A proper approximation would be rather sum of Gaussian distributions in both variables. It should be pointed out, that figure 4.3 presents only projections of joint probability distribution of both variables in particular times. The joint distribution is plotted in figure 4.4.

Although the EKF did not converge to the true state in the previous simulation, if an initial estimate approximates the initial state well, the EKF provides good results. In contrast, dependence between convergence of a particle filter and difference between the initial estimate and the initial state is not significant. These results are summarized in figure 4.5.

Intuitive idea of complexity and stability of a particle filter (the SIR_{opt} filter in our case) can be obtained from figure 4.6. Here, two realizations of ω during a

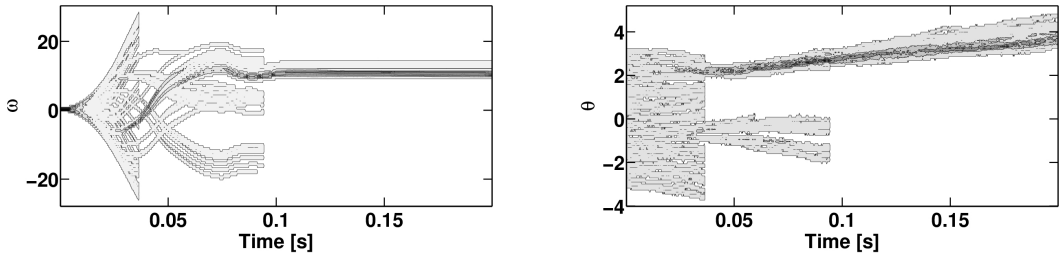

Figure 4.3: Estimated posterior distribution of ω and θ in particular times, the darker color means higher probability. Time steps, in which the resampling procedure was used, can be identified by sharp edges in estimates of posterior distribution.

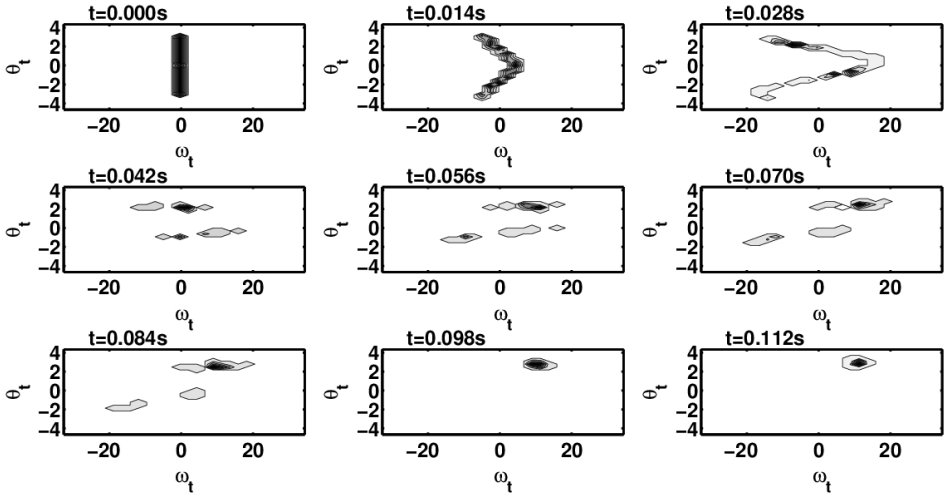

Figure 4.4: The joint distribution of ω and θ in particular times of the simulation, the darker color means higher probability. After the convergence of the estimate ($t > 0.112s$), ω stays on the desired value and θ is shifting due to the rotor motion.

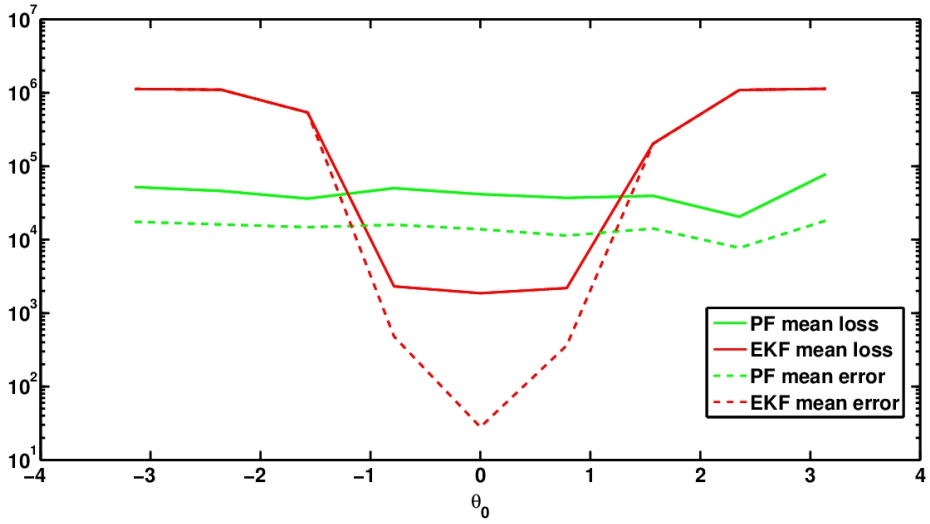

Figure 4.5: Dependence between initial θ and qulity of estimation. All the values are averages from 10 simulations.

simulation in which the initial state, initial estimate and system noise realization are the same. Differences are caused only by random realizations inside the particle filter. Note, that differences are amplified by the fact, that the control actions are based on different estimates.

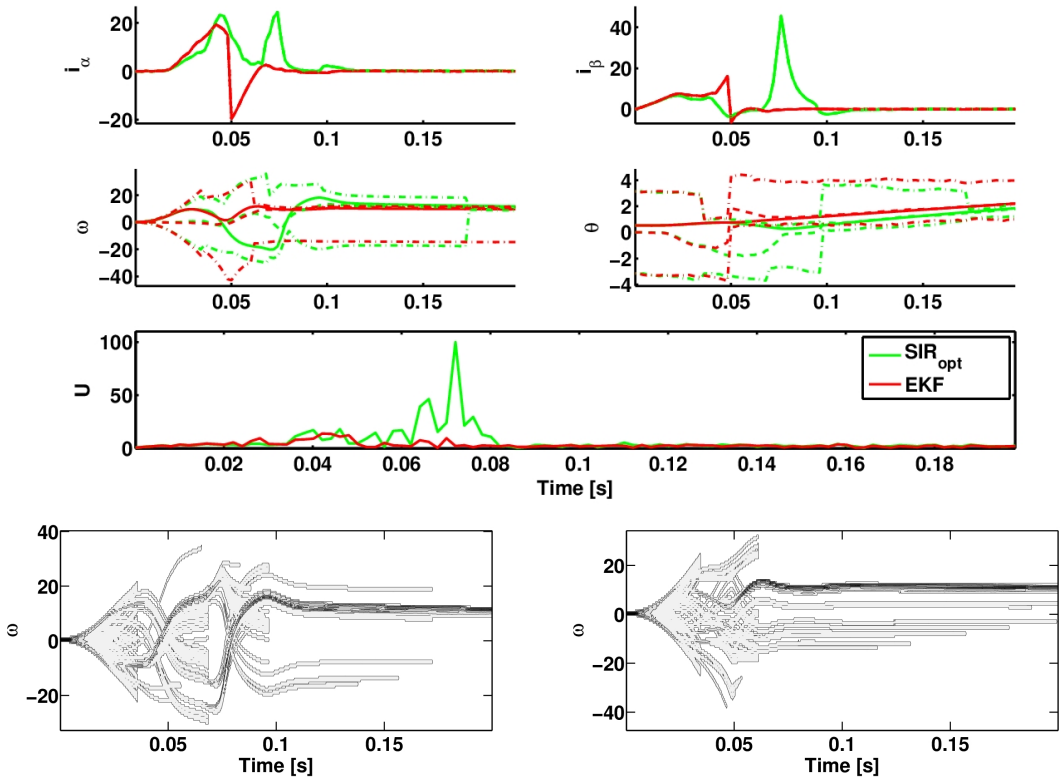

Figure 4.6: Two realizations of the same simulation using $\mathrm{SIR}_{\mathrm{opt}}$ filter. For ω_t and θ_t, the true state is marked by the full line, the estimate by the dashed line, and the bound of the estimated distribution by the dash-dot line. In histograms, the darker color means higher probability.

4.4.3 Qualitative comparison of control

This subsection deals with qualitative results of previously described regulators. The $\mathrm{SIR}_{\mathrm{opt}}$ filter with deterministic variant of residual resampling is used for filtering. Also, random realizations inside used filters are the same in all simulations.

Figure 4.7 shows results when different regulators are used. In the CEC and PI regulator, mean value of estimate is utilized for computing control action. As was mentioned at the end of subsection 4.3.2, having no additional information about the initial state, the CC regulator proposes control actions equal to zero. Due to this fact, the system will stay unchanged and the situation will be repeated in next time steps. As consequence, the CC regulator is unable to change the state. In practice, the state of the system is influenced by noise realizations and through this, the system will be deflected what (after a sufficiently long time) gives

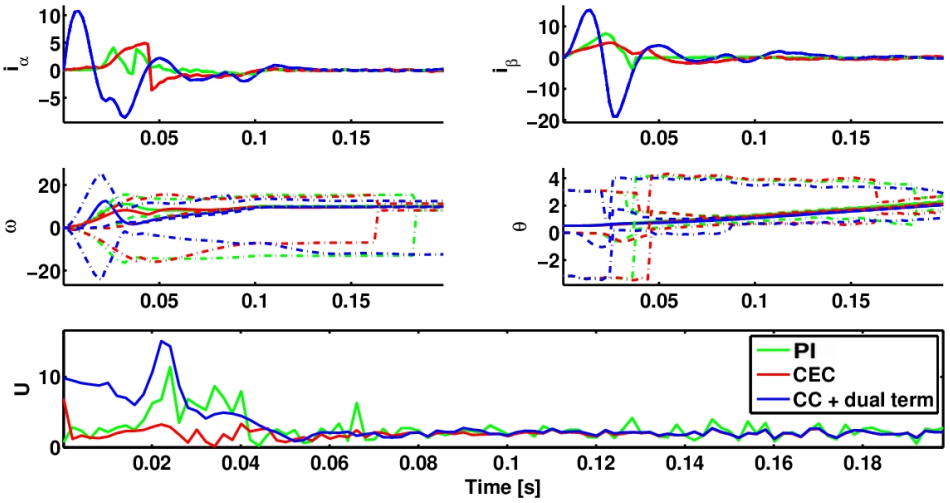

Figure 4.7: Qualitative comparison of different regulators. For ω_t and θ_t, the true state is marked by the full line, the estimate by the dashed line, and bound of the estimated distribution (in case of the SIR_{opt}) and the variance (in case of the KF) by the dash-dot line. The last figure shows the norm of control actions in respective times ($U = ||u||$).

an additional information which eliminates the zero control. From the figure, it can also be seen the advantage of incorporating the future effects of control action – although evolution of the state controlled by the CEC or PI regulator is nearly the same, the PI regulator proposes more aggressive control actions which yields into more rapid changes in currents without any valuable effect. As consequence, we assume that the controlling using the PI regulator will generate a higher loss. After reaching the desired state, regulators only compensate induced currents caused by the rotor motion.

The advantage of using the CC regulator with probing term can be viewed also from the following simulation. We assume a case in which the desired ω is zero during first 0.1s, then linearly increase during next 0.01s, and stays on 20 during last 0.2s. Comparison with the CEC regulator is shown in figure 4.8. In this case, $\hat{\omega}$ match with the desired value during first 0.1s. As consequence, CEC regulator proposes zero actions. In contradiction, the probing term in the CC regulator causes active learning during this phase. It results into more smooth controlling in future steps.

4.4.4 Quantitative results

In this section, quantitative results of proposed filters and estimators on the simulation of starting phase are presented. For better distinction between cases in which a particle filter (or a regulator) converged to a wrong value and cases where the estimation (or the regulation) only takes more time, we extend the second phase of the simulation, where the desired value of ω is kept constant, to 0.4s. The simulation is repeated 1000 times. In every single simulation, the initial state is drawn according

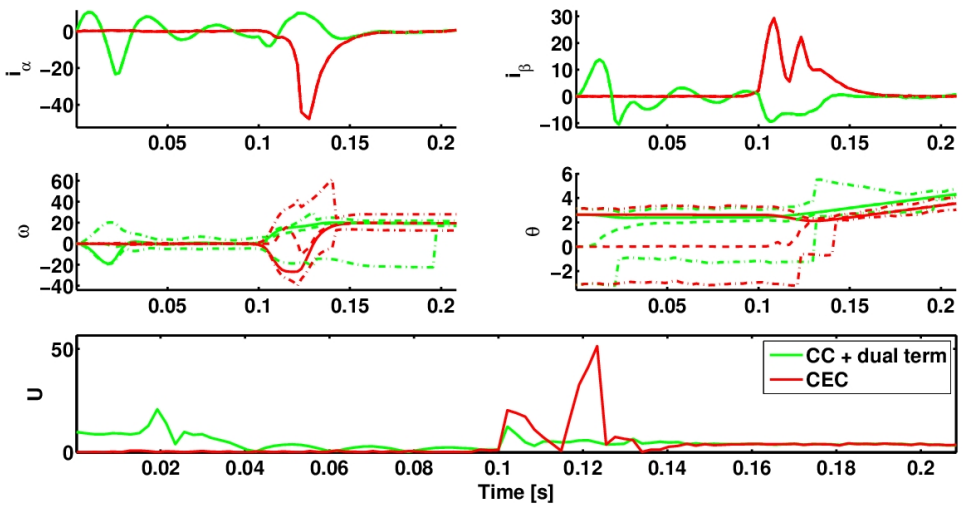

Figure 4.8: Comparison of the CC regulator with the probing term and the CE regulator in a case in which the initial $\hat{\omega}$ match with the desired value for first 0.1s.

to (4.71) and realizations of random variables are the same for all tested filters and regulators.

The quantitative comparison of previously discussed regulators is shown in figure 4.9. Obtained histograms states that the CC regulator with added probing term reach both the lowest tracking loss and estimation error. The most remarkable outline of the figure is that the amount of estimation failures significantly decreases, using the modified CC regulator. For the estimation, the SIR_{opt} filter with $N = 60$, $N_{thresh} = N/5 = 15$, and the deterministic variant of residual resampling is used.

As was mentioned before, if the SIR_{prior} and the ASIR filter are tuned properly, they propose nearly the same results as the SIR_{opt} filter, see 4.10. Similar results help us to tune the matrix $\tilde{R} = \rho R$ mentioned in previous text – we can see simulations in which estimation failed as those with estimation error $> 2.10^6$. Increase of robustness and thus decrease of the amount of failures can be done by increasing the ρ. However, the overall estimation error increases. Some compromise can be reached after some experiments with these histograms. Consequently, we use $\rho = 100$ for the SIR_{prior} filter and $\rho = 1000$ for the ASIR filter.

Computation limits for providing an estimate and a control action is very limiting (only $\Delta t = 0.000125$s), thus, an amount of particles in a particle filter should be small. Monte Carlo study for different number of particles is presented in figure 4.11. Here, the CC regulator with the probing term and the SIR_{opt} filter with the deterministic variant of residual resampling for $N_{thresh} = N/5$ are used.

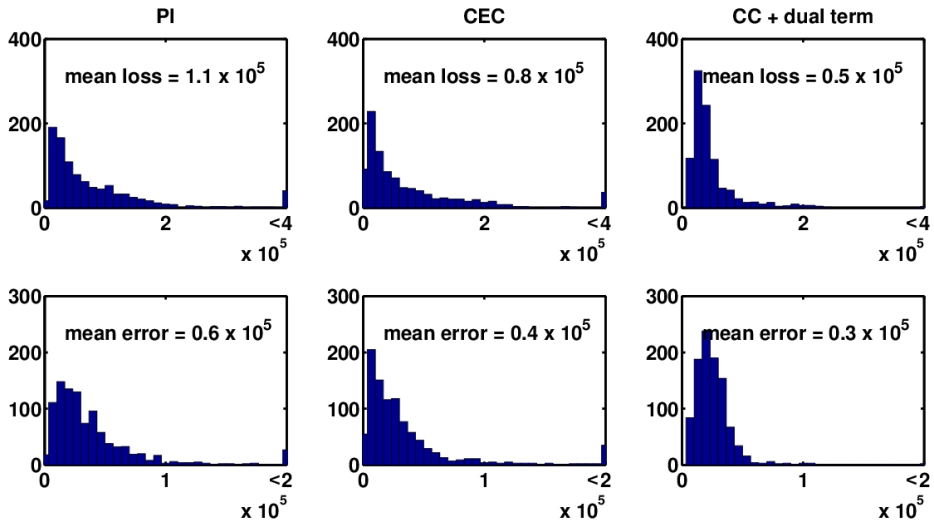

Figure 4.9: Qualitative comparison of different regulators.

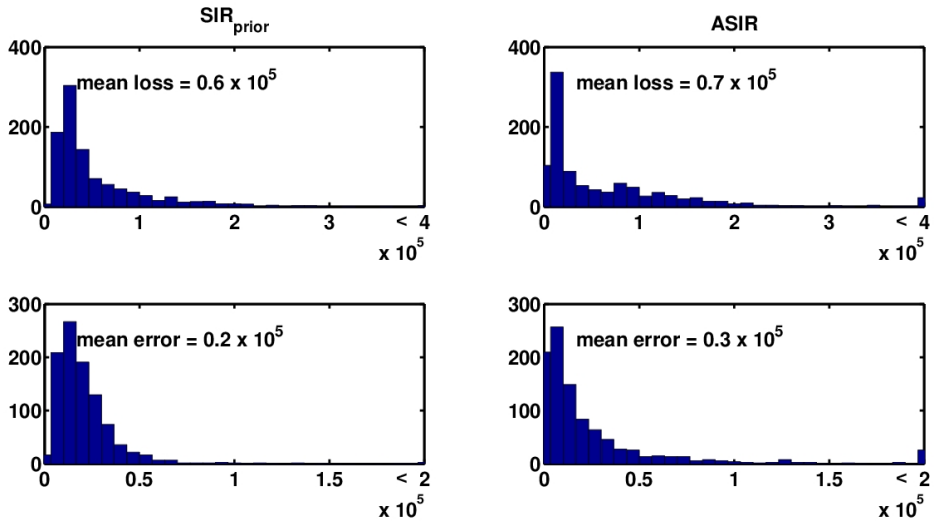

Figure 4.10: Qualitative comparison of different filters. Comparable results for the SIR_{opt} filter are shown in the first part of figure 4.9.

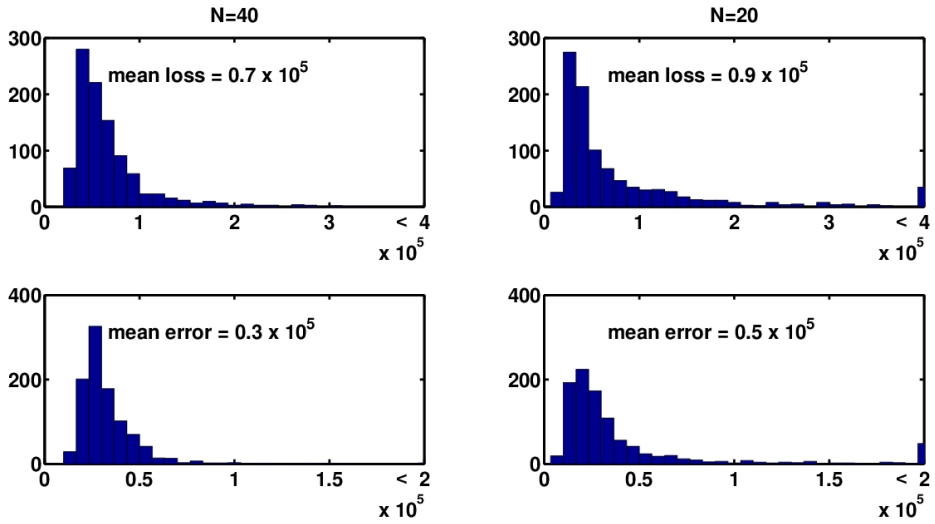

Figure 4.11: Tracking loss for different numbers of particles (= N). Results of the same simulation for $N = 60$ was shown in the last column of figure 4.9.

Conclusions

The scope of this research project was to study methods of particle filtering, especially in framework of controlling under uncertainty. Successful control should well identify hidden parameters of the system and, by some regulator, to propose control actions which yields into desired system state. The identify step can be viewed as sequential estimating problem and its solution using sequential Monte Carlo method was discussed. On the other hand, regulating step is a variant of minimization problem. The problem is often analytically unsolvable and, moreover, also its approximations based on some general idea like dynamic programming or gradient method are to time consuming. Consequently, we are often tended to use some more special regulators, e.g the PID, CEC or CC regulator.

After discussing the principles of estimating and controlling in control theory framework, we was interested in application of the methods on model of PMSM. For the system, several particles filters was implemented and compared with the EKF. The best estimation of posterior distribution was proposed by $\mathrm{SIR}_{\mathrm{opt}}$, however, also other particle filters proved to be able in estimating well. For controlling, the PI, CC and CEC regulator was implemented and tested. The CC and CEC regulators was outlined upon specific additional conditions which yield into simple and effective control law. During comparison, the most successful regulator was CC with added probing term. In addition, quantitative results proved that successful estimation can be achieved using only few particles.

Further research would be to utilize proposed estimation and controlling techniques on a PMSM model which would better match with real motor. Another direction would be to propose some general algorithm which would incorporate probing in controlling, less artificial than the presented one. One possibility could be to propose some extension of the SIDP or stochastic policy gradient algorithm which would be able to perform time consuming computations more effectively and offline.

References

[1] K.H. Ang, G. Chong, and Y. Li. PID control system analysis, design, and technology. *Control Systems Technology, IEEE Transactions on*, 13(4):559–576, 2005.

[2] M.S. Arulampalam, S. Maskell, N. Gordon, and T. Clapp. A tutorial on particle filters for online nonlinear/non-Gaussian Bayesian tracking. *Signal Processing, IEEE Transactions on*, 50(2):174–188, 2002.

[3] D.P. Bertsekas. *Dynamic Programming and Optimal Control, vol. 1*. Athena Scientific, 1995.

[4] C. Berzuini, N.G. Best, W.R. Gilks, and C. Larizza. Dynamical Conditional Independence Models and Markov Chain Monte Carlo Methods. *Journal of the American Statistical Association*, 92(440), 1997.

[5] S. Bolognani, L. Tubiana, and M. Zigliotto. Extended Kalman filter tuning in sensorless PMSM drives. *Industry Applications, IEEE Transactions on*, 39(6):1741–1747, 2003.

[6] R. Douc and O. Cappé. Comparison of resampling schemes for particle filtering. In *Image and Signal Processing and Analysis, 2005. ISPA 2005. Proceedings of the 4th International Symposium on*, pages 64–69. IEEE, 2005.

[7] A. Doucet, N. De Freitas, and N. Gordon. *Sequential Monte Carlo methods in practice*. Springer Verlag, 2001.

[8] A. Doucet, S. Godsill, and C. Andrieu. On sequential Monte Carlo sampling methods for Bayesian filtering. *Statistics and computing*, 10(3):197–208, 2000.

[9] A. Doucet and X. Wang. Monte Carlo methods for signal processing: a review in the statistical signal processing context. *Signal Processing Magazine, IEEE*, 22(6):152–170, 2005.

[10] VA Epanechnikov. Nonparametric estimation of a multidimensional probability density. *Teoriya Veroyatnostei i ee Primeneniya*, 14(1):156–161, 1969.

[11] A. A. Feldbaum. Dual control theory i-iv. *Automation and Remote Control*, 21,22:874–880, 1033–1039,1–12, 109–121, 1960,1961.

[12] P.W. Glynn and D.L. Iglehart. Importance sampling for stochastic simulations. *Management Science*, pages 1367–1392, 1989.

[13] T. Higuchi. Monte Carlo filter using the genetic algorithm operators. *Journal of Statistical Computation and Simulation*, 59, 1996.

[14] J.D. Hol, T.B. Schon, and F. Gustafsson. On resampling algorithms for particle filters. In *Nonlinear Statistical Signal Processing Workshop, 2006 IEEE*, pages 79–82. Ieee, 2007.

[15] A. Jasra and P. Del Moral. Sequential Monte Carlo methods for option pricing. *Arxiv preprint arXiv:1005.4797*, 2010.

[16] S.J. Julier and J.K. Uhlmann. A new extension of the Kalman filter to nonlinear systems. In *Int. Symp. Aerospace/Defense Sensing, Simul. and Controls*, volume 3, page 26. Citeseer, 1997.

[17] T. Hagglund K. J. Astrom. *PID Controllers:theory, Design, and Tuning*. The International Society for Measurement and Control, 1995.

[18] R.E. Kalman. A new approach to linear filtering and prediction problems. *Journal of basic Engineering*, 82(1):35–45, 1960.

[19] G. Kitagawa. Monte Carlo filter and smoother for non-Gaussian nonlinear state space models. *Journal of computational and graphical statistics*, 5(1):1–25, 1996.

[20] A. Kong, J.S. Liu, and W.H. Wong. Sequential imputations and Bayesian missing data problems. *Journal of the American Statistical Association*, 89(425):278–288, 1994.

[21] J.H. Kotecha and P.M. Djuric. Gaussian sum particle filtering. *Signal Processing, IEEE Transactions on*, 51(10):2602–2612, 2003.

[22] Z. Peroutka, V. Smidl, and D. Vosmik. Challenges and limits of extended Kalman Filter based sensorless control of permanent magnet synchronous machine drives. In *Power Electronics and Applications, 2009. EPE'09. 13th European Conference on*, pages 1–11. IEEE, 2009.

[23] M.K. Pitt and N. Shephard. Filtering via simulation: Auxiliary particle filters. *Journal of the American Statistical Association*, pages 590–599, 1999.

[24] D. Salmond, N. Gordon, and A. Smith. Novel approach to nonlinear/non-gaussian bayesian state estimation. In *IEE Proc. F, Radar and signal processing*, volume 140, pages 107–113, 1993.

[25] J.S. Simonoff. *Smoothing methods in statistics*. Springer Verlag, 1996.

[26] S.S. Singh, N. Kantas, B.N. Vo, A. Doucet, and R.J. Evans. Simulation-based optimal sensor scheduling with application to observer trajectory planning. *Automatica*, 43(5):817–830, 2007.

[27] A.M. Thompson and W.R. Cluett. Stochastic iterative dynamic programming: a Monte Carlo approach to dual control. *Automatica*, 41(5):767–778, 2005.

[28] P. Vas. *Electrical machines and drives: a space-vector theory approach*. Monographs in electrical and electronic engineering. Clarendon Press, 1992.

[29] D. Yuan, X. Cui, D. Fan, W. Feng, and Y. Yu. Application of Kalman Filter Method to the Date Processing of GPS Deformation Monitoring. In *2010 Second International Workshop on Education Technology and Computer Science*, pages 269–272. IEEE, 2010.